2018-07-01

# Deep-Tissue Heating as a Therapeutic Intervention to Prevent Skeletal Muscle Atrophy in Humans

Paul S. Hafen
*Brigham Young University*

# Deep-Tissue Heating as a Therapeutic Intervention to Prevent Skeletal Muscle Atrophy in Humans

Paul S. Hafen

A dissertation submitted to the faculty of
Brigham Young University
in partial fulfillment of the requirements for the degree of

Doctor of Philosophy

Robert Hyldahl, Chair
Pat Vehrs
Allen Parcell
Gary Mack
David Thomson

Department of Exercise Sciences

Brigham Young University

ABSTRACT

Deep-Tissue Heating as a Therapeutic Intervention to
Prevent Skeletal Muscle Atrophy in Humans

Paul S. Hafen
Department of Exercise Sciences, BYU
Doctor of Philosophy

Skeletal muscle is a highly adaptable tissue that comprises approximately 40% of total body weight while accounting for up to 90% of whole-body oxygen consumption and energy expenditure during exercise. The loss of skeletal muscle protein and subsequent decrease in muscle mass (atrophy) that accompanies disuse results primarily from a decrease in intracellular protein synthesis combined with an increase in proteolytic activity. Interestingly, these processes of skeletal muscle atrophy are amplified by changes in mitochondrial capacity, with evidence suggesting that the maintenance of mitochondria during periods of disuse protects skeletal muscle against atrophy. Remarkably, rodents with denervated muscle are protected against muscle atrophy following whole-body heat stress. The mechanism of protection appears to be tied to the observed increases in heat shock protein (HSP) and PGC-1α, which accompany the heat stress. Without any published observations as to whether such heat-induced protection against muscle atrophy would translate to human muscle, the aim of this project was to determine the extent to which deep tissue heating (via pulsed shortwave diathermy) might provide protection against skeletal muscle atrophy.

Keywords: muscle atrophy, human skeletal muscle, immobilization, heat stress, heat shock, mitochondrial respiration

Table of Contents

List of Tables

List of Figures

# Introduction

Skeletal muscle is a highly adaptable tissue that comprises approximately 40% of total body weight, while accounting for up to 90% of whole-body oxygen consumption and energy expenditure during exercise (5, 20). Furthermore, a substantial amount of research has shown that an adequate amount of muscle mass can prevent the development of several chronic diseases (e.g., type II diabetes and obesity) and is necessary to maintain work capacity throughout the lifespan (66, 86). While improvements in metabolic capacity, structure, and function of skeletal muscle occur in response to regular exercise training, these same characteristics are compromised during periods of physical inactivity or muscle disuse (33, 46).

The loss of skeletal muscle protein and subsequent decrease in muscle mass (atrophy) that accompanies disuse results primarily from a decrease in intracellular protein synthesis combined with an increase in proteolytic activity (33). Interestingly, these processes of skeletal muscle atrophy are amplified by changes in mitochondrial capacity, with evidence suggesting that the maintenance of mitochondria during periods of disuse protects skeletal muscle against atrophy (64). Remarkably, rodents with denervated muscle are protected against muscle atrophy following whole-body heat stress. The mechanism of protection appears to be tied to the observed increases in heat shock proteins (HSPs) and peroxisome proliferator-activated receptor gamma, coactivator-1 alpha (PGC-1α), which accompany the heat stress (75). While the increased HSPs provide more structural protection by preventing the breakdown of protein structures, PGC-1α maintains metabolic capacity by maintaining mitochondrial function. These potential mechanisms of protection are supported by transgenic animal research that has shown significant reductions in muscle atrophy with the overexpression of either PGC-1α (68), HSP27 (16), or HSP70 (70).

Heat-induced protection against muscle atrophy has not yet been shown in human skeletal muscle, as there is some controversy as to whether surface heating modalities (e.g., heating pad, hot water immersion, sauna) can raise muscle temperature sufficiently. For example, the use of superficial heating pads lead to robust temperature increases at a depth of 1 cm below the skin (~4°C), but only small increases (< 1°C) at depths approaching those of the deeper skeletal muscles (17). In order to address the limitations related to heating depth, we will use a common therapeutic modality of deep tissue heating called pulsed-shortwave diathermy. Pulsed-shortwave diathermy uses nonionizing electromagnetic waves to produce significant temperature changes (~3 to 4°C) at greater depths (~3 to 3.5 cm) than superficial heating pads (18).

With the ability to change intramuscular temperatures deep within skeletal muscle, we will test the concept of heat-induced protection against muscle atrophy in human skeletal muscle. It has been shown that 10 days of immobilization is sufficient to decrease muscle cross-sectional area (12%) and muscle strength (−40%) in human skeletal muscle (78). Therefore, to assess the effect of heat stress on skeletal muscle function and structure in the face of muscle wasting, we employed daily deep tissue heating during a 10-day immobilization timeline.

Specific Aims and Hypotheses

*Specific Aim I.* To determine the effect of daily deep tissue heating (2 hours/day) on the maintenance of metabolic capacity in response to 10 days of unilateral lower limb immobilization.

i. We hypothesized that repeated deep tissue heating would attenuate the loss of mitochondrial respiratory capacity (OXPHOS and ETS) in skeletal muscle subjected to immobilization.

ii. We hypothesized that repeated deep tissue heating would attenuate the loss of mitochondrial respiratory chain complex proteins (Complexes I, II, III, IV, and V) in skeletal muscle subjected to immobilization.

*Specific Aim II.* To determine the effect of deep tissue heating (2 hours/day) on the maintenance of muscle size in response to 10 days of unilateral limb immobilization.

i. We hypothesized that deep tissue heating would lead to decreased levels of the intracellular proteins (MAFbx, Murf1) involved in the muscle atrophy processes. Specifically, we expected to observe lower changes in MAFbx and Murf1 expression in skeletal muscle treated with deep tissue heating.

ii. We hypothesized that deep tissue heating would attenuate the muscle atrophy from 10 days of immobilization as measured by whole muscle (magnetic resonance imaging) and fiber (immunohistochemistry) cross-sectional area.

## Study 1

## Repeated Exposure to Heat Stress Induces Mitochondrial Adaptation in Human Skeletal Muscle

### Abstract

The heat stress response is associated with several beneficial adaptations that promote cell health and survival. Specifically, in vitro and animal investigations suggest that repeated exposures to a mild heat stress (~40°C) elicits positive mitochondrial adaptations in skeletal muscle comparable to those observed with exercise. To assess whether such adaptations translate to human skeletal muscle, we produced local, deep tissue heating of the vastus lateralis via pulsed shortwave diathermy in 20 men (n = 10) and women (n = 10). Diathermy increased muscle temperature by 3.9°C within 30 minutes of application. Immediately following a single 2-hour heating session, we observed increased phosphorylation of AMPK and ERK1/2, but not

of p38 MAPK nor JNK. Following repeated heat exposures (2 hours daily for 6 consecutive days), we observed a significant cellular heat stress response, as heat shock protein 70 and 90 increased 45% and 38%, respectively. In addition, the expression of PGC-1α and mitochondrial respiratory protein Complexes I and V were increased after heating. These increases were accompanied by augmentation of maximal coupled and uncoupled respiratory capacity measured via high-resolution respirometry. Our data provide the first evidence that mitochondrial adaptation can be elicited in human skeletal muscle in response to repeated exposures to mild heat stress.

Introduction

Mitochondria are responsible for the aerobic transformation of cellular energy, and their optimal function is vital to human health. Declines in mitochondrial content and function are central to the pathophysiology of many of the 21$^{st}$ century's most prominent health burdens including cardiovascular disease and type II diabetes (29, 66). Maintenance of skeletal muscle mitochondrial function through the lifespan is dependent on adaptations to repeated perturbations in cell homeostasis. The most studied of these perturbations is physical activity, which provides many well-documented benefits to both skeletal muscle and whole-body health (30, 31). Unfortunately, many diseased states that are associated with mitochondrial deficits (e.g., COPD, type II diabetes, cancer cachexia, sarcopenia) also demonstrate a concomitant intolerance to exercise, making it more difficult to correct any underlying mitochondrial deficiencies. Thus, development of complementary interventions aimed at eliciting the beneficial adaptations associated with exercise training are needed (66, 67).

During physical exercise, working muscles are exposed to many stresses resulting from increased muscle contractile activity and greater energetic demand. One of these stresses is a

change in temperature, which increases with both work intensity and metabolic rate (8, 67). As opposed to being a mere byproduct of increased muscle activity, the production of heat may represent an exercise-associated stress capable of eliciting beneficial muscular adaptations. For instance, exposure of cultured muscle cells to a moderate heat stress (~40°C) increases the expression of both the protective heat shock proteins (HSPs) and the transcriptional coactivator peroxisome proliferator-activated receptor gamma, coactivator-1 alpha (PGC-1α), a key regulator of mitochondrial biogenesis. Consequently, daily heat treatments administered to cultured muscle cells increases mitochondrial content in as little as one week (44). Similarly, rodents subjected to daily, whole-body heat stress express higher mitochondrial enzyme activity and protein content within their skeletal muscle. Moreover, when whole-body heat stress is administered immediately following exercise training, the adaptations are even more pronounced (76). Thus, repeated heat stress appears to be a possible strategy to increase mitochondrial content in skeletal muscle for those who are either limited in their exercise capacity or who are unable to exercise.

Despite the growing body of evidence from in vitro and animal research, heat-induced mitochondrial adaptations have yet to be confirmed in human skeletal muscle. Therefore, our primary objective was to determine whether repeated exposure to heat stress (REHS), much like repeated bouts of exercise, would be sufficient to stimulate mitochondrial adaptation in human skeletal muscle. Further, we explored potential cellular mechanisms that may mediate heat-induced mitochondrial adaptive mechanisms in human skeletal muscle.

## Methods

**Study description**. Twenty healthy, sedentary volunteers (10 male, 10 female) participated in the study. Characteristics of the participants are provided in Table 1.1. Subjects

were considered healthy, as they reported no signs/symptoms of cardiovascular or metabolic disease. Additionally, the subjects had not been actively participating in regular exercise training during the preceding 3 months. The Brigham Young University Institutional Review Board approved this study. Each volunteer was informed of the purpose of the study, experimental procedures, and potential risks associated with the study before written consent was obtained.

**Muscle heating and study design**. A schematic representation of this study protocol is provided in Figure 1.1. The leg of each volunteer was randomly assigned to serve as either the control or heat-assigned limb for the duration of the study. On the first visit, a 20-gauge, 1.88-in catheter (BD Medical, Sandy UT) was inserted approximately 3.5 cm into the vastus lateralis muscle of the heat-assigned quadriceps. A small thermocouple (IT-21; Physitemp Instruments, Clifton NJ) was inserted through the catheter, after which the catheter was removed and intramuscular temperature was relayed from the thermocouple to an Iso-Thermex electrothermometer (Columbus Instruments, Columbus OH). The thermocouple was only inserted into the muscle of the heat assigned leg in order to confirm changes in muscle temperature. The insertion was approximately 3 to 4 cm below the location marked for the first biopsy in order to minimize any confounding effects of the needle insertion from our biopsy sample. Furthermore, the thermocouple was only inserted on the initial heating visit to avoid any potential perturbations from repeated needle sticks. Following the insertion of the thermocouple, the quadriceps were heated for 2 hours using pulsed shortwave diathermy (Megapulse II, Accelerated Care Plus, Reno NV) at 800 pulses per second and with a pulse duration of 400 μsec. Immediately following (~10 to 15 minutes) the acute heating session, muscle biopsies were obtained from the vastus lateralis of both the control and heated quadriceps muscles. Each participant was given 3 days to allow the incision sites of the biopsies to close, after which the 6-

day heat treatment program was initiated (2 hours per day/6 consecutive days). Twenty-four hours following the final heating session, biopsies were taken from the vastus lateralis of both the control and heated quadriceps.

**Muscle biopsy protocol**. Percutaneous needle biopsies were taken from the vastus lateralis muscle of the quadriceps of both legs. The first biopsies were taken from both the control and heated legs on day 1, then again 24 hours after the completion of a 6-day heat treatment program. Under local anesthesia (2% lidocaine with epinephrine), a small incision was made into the skin and fascia. A Bergström biopsy needle was inserted into the muscle and, with the use of manual suction, a small 80 to 100 mg sample of tissue was withdrawn. Samples were then separated from fatty tissue and divided into 20 to 40 mg portions. Portions designated for protein and enzymatic analyses were frozen immediately in liquid nitrogen and stored at −80°C. Smaller portions (8 to 10 mg), designated for respirometry, were placed in ice-cold *buffer X* (60 mM K-MES; 35 mM KCl; 7.23 mM $K_2$EGTA; 2.77 mM $CaK_2$EGTA; 20 mM imidazole; 0.5 mM DTT; 20 mM taurine; 5.7 mM ATP; 15 mM PCr; and 6.56 mM $MgCl_2$). These portions were kept on ice, and respiration analyses were completed within 1 to 2 hours after collection.

**Mitochondrial respiration**. Measurements of skeletal muscle mitochondrial respiration were performed on permeabilized fibers using a Clarke oxygen electrode high-resolution respirometer (Oxygraph O2k, Oroboros Instruments, Innsbruck AUT). Using fine-tipped forceps, fibers were gently separated (teased) from one another to maximize surface area of the fiber bundle with only small portions connected to ensure that fibers were not disconnected or lost during permeabilization. Following teasing, fibers were carefully dried on fresh filter paper and weighed before being placed in ice-cold *buffer X*. The measurement of sample dry weight allowed respiratory measures to be normalized between runs and accounted for potential

differences in chamber loading. Fibers (3 to 6 mg) were then permeabilized with the addition of saponin to a final concentration of 50 µg/ml. To assess mitochondrial respiratory capacity, we followed a standard substrate-uncoupler-inhibition-titration (SUIT) protocol, allowing us to assess individual components of the respiratory chain (25). All respiratory experiments were carried out in MiRO5 buffer (110 mM sucrose; 60 mM potassium lactobionate; 2 mM magnesium Chloride; 20 mM taurine; 10 mM potassium phosphate; 0.5 mM EGTA; 20 mM HEPES; and 1 g/L BSA) at 25°C with spinning at 750 rpm. Oxygen concentrations were maintained between 500 and 200 µM throughout each experiment.

The SUIT protocol began with the addition of glutamate (10 mM) and malate (2 mM). After allowing for steady-state reading of oxygen uptake in the presence of glutamate and malate (leak), ADP (2.5 mM) was added to drive respiration through Complex I ($P_I$; CI). Following the measurement of CI-mediated respiration, cytochrome c (10 µM) was added to confirm integrity of the outer mitochondrial membrane. Stimulation of respiration by added cytochrome c would indicate injury to the membrane. We did not observe a positive cytochrome c response in any of our samples permeabilized with saponin. Following confirmation of intact mitochondrial membranes, succinate (10 mM) was added to stimulate respiration through Complex II ($P_{I+II}$; CII). Thus, we were able to measure maximal coupled respiration (OXPHOS) as both CI and CII were contributing to the total oxygen flux. Maximal uncoupled respiratory capacity (E; ETS) was then assessed with the addition of the uncoupler FCCP (2 to 3 steps of 0.125 µM FCCP). The response following the addition of FCCP demonstrates the limits of the phosphorylation system observed from OXPHOS. After measuring ETS, rotenone (0.5 µM) was added to inhibit CI, so that only CII could be contributing to the uncoupled respiration processes. Finally, residual oxygen consumption (ROX) was measured following the addition of Antimycin A (2.5 µM) to

inhibit Complex III. ROX was subtracted from oxygen flux as a baseline for all respiratory states.

**Protein immunoblotting**. Whole muscle was homogenized in chilled Mitochondria Lysis Buffer (EMD Millipore, Bedford MA), with added phosphatase and protease inhibitors (Thermo Fisher Scientific), at a volume of 9 µl per 1 mg tissue. Homogenates were centrifuged at 600*g*, and the supernatants were transferred to clean tubes and stored at −80ºC. Protein concentration was determined using a Pierce™ Bicinchonic Acid (BCA) Kit (Thermo Fisher Scientific, Waltham MA) and spectrophotometer (Victor3™, Perkin Elmer, Waltham MA), according to the manufacturer's specifications. Samples were diluted with 2x loading buffer to a concentration of 1 µg/µl (20 ug total) and ran on a 4 to 15% graded SDS-polyacrylamide gel (Bio-Rad, Hercules CA) at 200 V for 50 minutes at room temperature. All samples from each subject were run on the same gel to avoid any variability between gels. Following electrophoresis, proteins were transferred to a PVDF membrane at 100 V for 60 minutes at 4ºC. Membranes were blocked in 5% milk diluted in tris-buffered saline with Tween (TBST) for 60 minutes at room temperature. Following blocking, membranes were incubated in primary antibodies diluted in 5% bovine serum albumin (BSA) in TBST for either pAMPK (1:5000; Cell Signaling, Danvers MA), or PGC-1α (1:1000; EMD Millipore, Bedford MA) overnight at 4ºC. Each membrane was then washed in TBST and probed with either anti-mouse or anti-rabbit secondary antibodies (1:10,000; Santa Cruz Biotech). The bands of interest were then exposed through chemiluminescence (ECL) and imaged using ChemiDoc XRS (Bio-Rad, Hercules CA) CCD high-resolution, high-sensitivity technology. Following imaging, the pAMPK membranes were incubated in stripping buffer (0.2 M glycine, 10% tween, 0.1% SDS, 2.2 pH) and NaOH (0.2 M), then re-blocked in 5% milk in TBST for 60 minutes at room temperature. The stripped

membranes were reprobed with secondary antibody, exposed using ECL, and viewed using a ChemiDoc XRS camera to confirm stripping. The membranes were then rewashed, and reincubated in primary antibodies for total AMPK (1:4000; Cell Signaling, Danvers MA), the bottom portion of the PGC-1α membranes were incubated in antibody against Glyceraldehyde 3-phosphate Dehydrogenase (GAPDH; 1:2000; Santa Cruz Biotech, Dallas TX) overnight at 4ºC. Each membrane was washed in TBST and probed with either anti-mouse or anti-rabbit secondary antibodies (1:10,000; Santa Cruz Biotech, Dallas TX). Imaging proceeded as described for the pAMPK and PGC-1α membranes. Data were normalized to account for potential variations in loading by using the ratios for pAMPK/total AMPK and PGC-1α/GAPDH.

**Magnetic bead multiplex**. The Magpix (Luminex, EMD Millipore, Burlington MA) multiplexing platform was used to assess MAPK phosphorylation, HSP and mitochondrial protein content of biopsy sample homogenates. All samples from each subject were measured on the same plate in order to account for any variability that might be present between different plates. MAPK phosphorylation was measured using a 9-plex multipathway total magnetic bead kit (EMD Milliplex® MAP, Cat. # 48-680MAG, Burlington MA). Specifically, 25 µg of protein homogenate were incubated in antibody-conjugated magnetic beads overnight at 4°C. The bead complex was then washed, followed by a 1-hour incubation at room temperature (RT) on a plate shaker in biotinylated detection antibody. Streptavidin-phycoerythrin was subsequently added and samples were incubated for an additional 30 minutes on a plate shaker at RT.

HSP content was measured using a 5-plex HSP magnetic bead kit in compliance with manufacturer's parameters (EMD Milliplex® MAP, Cat. # 48-615MAG, Burlington MA). Specifically, 150 ng of protein homogenate were incubated overnight at 4°C with antibody-

conjugated magnetic beads. The bead-complex was then washed, followed by a 1-hour incubation at RT on a plate shaker in biotinylated detection antibody. Streptavidin-phycoerythrin was subsequently added and samples were incubated for an additional for 30 minutes on a plate shaker at RT.

Mitochondrial protein content was measured using a human oxidative phosphorylation magnetic bead panel (EMD Milliplex® MAP, Cat. # HOXPSMAG-16K, Burlington MA). Specifically, 20 µg of protein homogenate were incubated in antibody-conjugated magnetic beads for 2 hours at RT. The bead-complex was then washed, followed by a 1-hour incubation in biotinylated detection antibody. Streptavidin-phycoerythrin was added for an additional 30-minute incubation period.

A Magpix (Luminex Corporation, Austin, TX) system was used to quantify bead-complexes for each of the 3 multiplex protocols. Data analyses were completed using median fluorescence values for each of the bead-complexes.

**Citrate synthase (CS) maximal activity**. Citrate synthase activity was measured via spectrophotometric enzyme analysis, according to the procedures developed by Spinazzi et al. (74). Briefly, frozen muscle samples were homogenized at a concentration of 1:20 in ice-cold sucrose muscle homogenization buffer (250 mM). Following homogenization, samples were centrifuged and the supernatant was transferred into a new Eppendorf tube for the CS analysis. A 10-µl aliquot was used to measure total protein concentration for each sample, via BCA analysis as previously described. All analyses were completed on the same day as homogenization. For the measurement of CS activity, each well of a 96-well plate was loaded with 184 µl of 200 mM Tris buffer (0.2% Triton-X), 2 µl of supernatant, 2 µl 10 mM DTNB, and 2 µl of 30 mM acetyl-CoA. Triplicate measures were taken for each sample. Baseline absorbance was measured every

30 seconds for 2 minutes at 412 nm. After attaining baseline absorbance, 10 µl of ×10 mM oxaloacetic acid was added and the measurement process repeated (every 30 seconds for 2 minutes at 412 nm).

**Statistics**. A mixed-models analysis of variance (ANOVA) was used in order to examine the main effects of time (pre vs post) and condition (treatment vs control) on the dependent variables. With a significant time × condition interaction, individual comparisons over time, or between conditions, were explored using student *t*-tests. When analyzing acute phosphorylation, only dependent *t*-tests were performed as there was not a time component when comparing these events between the acute tissue samples. Analyses were completed using JMP® Pro SAS statistical software, version 13.0. Alpha was set a priori at $p < 0.05$. Data are expressed as means ± SEM.

Results

**Intramuscular temperature**. Muscle temperature during pulsed shortwave diathermy increased 3.9 ± 0.31°C ($p < 0.0001$) by 30 minutes, where it plateaued, and remained elevated over the remaining 1.5-hour heating duration (Figure 1.2).

**Cellular signaling**. We first sought to determine whether the change in temperature was associated with acute phosphorylation events related to cellular stress and mitochondrial biogenesis. For this we compared differences between the heat-assigned leg and the nonheated control leg immediately following a single 2-hour heating session. We observed a decrease in the phosphorylation of HSP27 (25 ± 7.8%, $p = 0.0012$, Figure 1.3) relative to the control leg. The total concentrations of other HSP proteins were unaltered immediately following the first heating session (Figure 1.4), most likely due to the early sampling period (immediately following the heating session) of the initial biopsies.

While a variety of stresses appear capable of initiating mitochondrial biogenesis (31, 66), heat exposure in vitro has been associated with increases in AMP-activated protein kinase (AMPK) activity (44), whereas whole-body heat stress in rodents appears to increase PGC-1α expression via activation of p38 mitogen-activated protein kinase (p38 MAPK) (76). Based on these reported observations, we explored the potential of heat stress to induce changes in the phosphorylation state of AMPK and several well-studied MAPKs. Immediately following the acute 2-hour heating session, significant elevations were observed in the phosphorylation of AMPK (32 ± 15.8%, $p = 0.0365$) and extracellular signal-regulated kinase 1/2 (ERK1/2) (205 ± 74.8%, $p = 0.0246$) relative to the control leg. No significant changes in the phosphorylation of p38 or JNK were observed (Figure 1.3).

**HSP expression**. Protein expression of HSPs were not changed immediately following a single bout of heating (Figure 1.4). However, following REHS, expression of the major heat-inducible HSP70 increased 45 ± 18.8% ($p = 0.0003$). In addition, HSP90 content increased 38 ± 13.4% ($p < 0.0001$). In contrast, REHS did not affect total protein expression HSP27 or HSP60 (Figure 1.4).

**Mitochondrial biogenesis**. To ascertain whether the heating intervention resulted in de novo synthesis of mitochondria, we assessed mitochondrial biogenesis using a multiparameter approach (40). We measured the concentrations of the 5 mitochondrial respiratory chain proteins (Complex I, II, III, IV, and V), PGC-1α protein content, and maximal enzymatic activity of citrate synthase (CS). Following REHS, increases in the expression of mitochondrial protein Complex I (37 ± 19.0%, $p = 0.0281$) and V (39 ± 22.4%, $p = 0.0461$) were observed in the muscle from the heated leg (Figure 1.5). In addition, PGC-1α protein content was 10 ± 3.3%

higher in the heated muscle (Figure 1.6, $p = 0.0461$). However, maximal CS activity did not change in response to REHS (Figure 1.6).

**Mitochondrial function**. Respiratory capacity was not changed immediately following an acute bout of heating (Figure 1.7). However, following REHS, CI-mediated respiration (GMSp) was 28 ± 10.3% higher, OXPHOS was 28 ± 10.7% higher ($p = 0.0175$) and ETS increased in similar magnitude (29 ± 10.6%, $p = 0.0084$). CII-mediated uncoupled respiration (S[Rot]e) was not changed following heating (Figure 1.7).

To determine whether this effect could be attributed to changes in mitochondrial respiratory efficiency, we examined the relationship between absolute changes in OXPHOS relative to changes in ETS. The observed changes in OXPHOS correlated very strongly ($r = 0.94$, $p < 0.0001$) to changes in ETS. Also, the P/E coupling control ratio (OXPHOS/ETS), which estimates the limitation of the phosphorylation system on maximal respiratory capacity, was not affected by REHS ($p = 0.1979$, Figure 1.7), despite the increased maximal respiratory capacity. Thus, the higher capacity observed in the heated muscle appeared to be the result of increased capacity within both the phosphorylation and electron transfer systems as opposed to alterations in mitochondrial efficiency.

## Discussion

Nearly 2 decades ago Hooper (32) showed that 10 days of repeated whole-body heating improved mean plasma glucose and glycosylated hemoglobin levels in type II diabetics, providing one of the first proof-of-principle studies on the potential clinical benefits of repeated whole-body heat stress. More recently, rodent studies have shown that repeated whole-body heat stress is capable of inducing mitochondrial biogenesis in skeletal muscle (76). Further, animals that overexpress heat shock proteins (HSP72) have an increased mitochondrial number, oxidative

capacity and improved insulin sensitivity (27). In this study, we hypothesized that a repeated, muscle-targeted heating approach would induce expression of heat shock proteins, drive the cellular signaling events associated with mitochondrial biogenesis, and improve mitochondrial respiratory capacity in human vastus lateralis. Indeed, our data indicate that repeated exposure to heat stress (REHS) increases both coupled and uncoupled mitochondrial respiratory capacity. Though others have used surrogate measures of mitochondrial function following heat stress (e.g., citrate synthase, Mt DNA copy number) in animals, these are the first data to report significant increases in mitochondrial function in human skeletal muscle following REHS. Complementary to these data, we also found increased protein content of Complex I, Complex V and PGC-1α, which suggest that in addition to improving function, REHS increased mitochondrial content in human skeletal muscle. However, we were unable to measure a change in citrate synthase (CS) activity, a common surrogate marker of mitochondrial content. Previous studies have shown that it is not uncommon to measure altered mitochondrial capacity and/or function in the absence of changes in CS activity (51, 61). Furthermore, it is highly unlikely that CS is limiting for mitochondrial function in healthy skeletal muscle, as its maximal activity is 10-fold higher than the maximal Krebs cycle rate (4). While the CS data do raise the question of whether the REHS protocol employed by this study actually altered mitochondrial content, our observed increases in respiratory chain proteins and respiratory capacity provide strong evidence that repeated heat stress is capable of improving muscle mitochondrial function.

Our REHS protocol (2 hours/day for 6 days) was based loosely on the minimum dose of submaximal exercise necessary to measure changes in muscle respiratory capacity (73). In a thermal neutral environment, quadriceps muscle temperature rises rapidly (~10 to 20 minutes) after initiation of submaximal exercise and plateaus at approximately 39°C (67). To mimic the

effects of exercise-induced muscle heating, we sought to achieve similar temperature changes using an externally applied modality. We found that pulsed shortwave diathermy, used at a wavelength of 27.12 MHz and at 800 bursts per second, very effectively mimicked the temperature changes observed during exercise, at the approximate depth of our muscle biopsy procedure (~3 to 3.5 cm). Further, pulsed shortwave diathermy has been previously shown to increase intramuscular HSP expression 24 hours posttreatment in human muscle (80). We show that a single, 2-hour diathermy treatment was sufficient to alter the phosphorylation of HSP27, yet we did not detect increases in HSP protein expression at our sampling point immediately postheating. However, it is not likely that we would be able to measure changes at the protein level so soon following the heating intervention. On the other hand, HSP70 and HSP90 protein content were markedly increased in the muscle at the end of the REHS protocol. Because our biopsies were taken 24 hours following the final heating session, it is impossible to say whether this was a chronic increase due to repeated heating or an acute effect brought about by a single heating session. While robust increases in HSP expression have been described extensively in skeletal muscle following both exercise and heating (38, 70, 81), there is limited evidence of their role in mediating mitochondrial adaptations. Barone et al. (3) showed that overexpression of HSP60 (not changed in our study) in cultured myoblasts induces PGC-1$\alpha$ expression, and HSP70 overexpressing mice appear resistant to age-related muscle dysfunction (48) and exercise-induced fatigue (43). Nevertheless, a mechanistic link between HSP70 or HSP90 expression and mitochondrial adaptation in muscle has yet to be fully characterized.

To further interrogate the potential mechanisms whereby heating may promote mitochondrial adaptation, we also assessed the cell signaling response to a single heat treatment. Several signaling pathways have been shown to influence mitochondrial biogenesis in humans

following exercise, the most well-studied being $Ca^{2+}$/calmodulin-dependent kinases (CaMKs) (58), p38 MAPK (2) and AMP-activated protein kinase (84). As our heat treatments did not involve active muscle contractions, and rodent studies have shown that whole-body heat treatments do not affect CaMKII phosphorylation (76), we focused on activity of AMPK and the MAPKs. Phosphorylation of AMPK increased significantly following 2 hours of muscle heating. This result confirms in vitro findings (44), but is in contrast to rodent whole-body heating, which appears to decrease AMPK activity in skeletal muscle (76). However, whole-body heating likely involves a greater systemic response than would be present with our targeted approach, making comparisons of these distinct models difficult. Nevertheless, it is relevant to point out that skeletal muscle AMPK activity is sensitive to a variety of tissue stressors including: hypoxia (47), calorie restriction (9), oxidative stress (88), and cold exposure (54). Thus, AMPK represents a potentially important intracellular mediator of heat-induced mitochondrial adaptation in humans. Quite unexpectedly, we found that phosphorylation of ERK1/2, but not p38 MAPK, was elevated in response to the 2-hour heat treatment in the heated leg, relative to the nonheated control leg. In nonmuscle cells, heat shock (42°C) has been shown to activate ERK MAPKs in a potent and sustained manner (57). Whether or not ERK1/2 phosphorylation is an important event for heat-induced mitochondrial biogenesis remains to be seen. Nevertheless, studies in cultured muscle cells suggest that translocation of ERK to mitochondria are important in mitochondrial stabilization during oxidative stress (65). Further work to determine the cellular mechanism for heat-induced skeletal muscle mitochondrial adaptation will provide important insights into the regulation of mitochondrial adaptation and vitality, which may have clinical significance.

Lastly, we found that an acute bout of muscle heating decreased phosphorylation of HSP27. Phosphorylation of HSP27 has not been particularly well-studied in the context of skeletal muscle adaptation, yet it has well-defined roles in assisting protein folding, actin cytoskeleton remodeling, oxidative stress reduction and inhibition of apoptosis in a host of other tissues (28, 83). In muscle, Kim et al. (37) showed that phosphorylation of HSP27 was significantly increased in the atrophied gastrocnemius of cast immobilized rats and serum starved L6 myotubes. In line with these data, transgenic cardiomyocytes with nonphosphorylatable HSP27 display much lower levels of oxidative stress (72). As heat stress, much like exercise, alters redox balance in skeletal muscle (50), it is possible that the increase in nonphosphorylated HSP27 observed in our study plays a role in redox balance during acute heat stress.

While the design of the study allowed us to assess both acute cellular signaling and chronic adaptation to REHS, there remain several limitations to the study that may hopefully be addressed with continued research on this topic. First, we did not take any measurements of core temperature to confirm the presence, or lack thereof, of a systemic response to the heating protocol. However, based on the consistency of our control measures between time points, it is unlikely that a systemically driven mechanism contributed to our observations. Second, we did not record temperature in the control leg. Although we did not gather temperature data from the control leg, we did attempt to minimize any confounding effect of the needle insertion by inserting the probe 3 to 4 cm distally from the marked biopsy site (see Methods). Finally, as part of our investigation into changes in protein expression, we analyzed the data to identify changes from pre-REHS to post-REHS. The timing of our premeasures was chosen to provide us with acute cellular signaling data, while also serving as the baseline assessment for potential adaptations following REHS. Our justification for this was our belief that the early timing of our

biopsies (taken immediately after a single heating session) would be sufficient to assess changes in acute cellular signaling while not affecting expression of the proteins of interest. In support, we found no differences in protein expression or respiratory capacity between legs following the initial 2-hour heating session (Acute).

In conclusion, we showed that repeated exposure to heat stress was sufficient to improve human skeletal muscle mitochondrial function and increase markers of mitochondrial biogenesis. Further, we showed that heat stress acutely increased AMPK and ERK1/2 phosphorylation, providing evidence that they may be involved in mediating heat-induced mitochondrial adaptation. The results of the study have clear and potentially far-reaching clinical implications. While exercise interventions currently represent the most effective strategy to prevent and treat metabolic disorders and improve fitness, many patients for whom exercise-based therapy would be most beneficial are either unable to exercise (i.e., immobilization postsurgery, on bed rest) or have very low tolerance for exercise (i.e., aged, obese, diseased populations). Importantly, pulsed shortwave diathermy is a safe and reliable modality that has been used as an injury recovery tool in humans for over a century. Our data provide evidence to support further research into the mechanisms of heat-induced mitochondrial adaptations and optimization of heating dose and duration. Given that such units can already be found in many rehabilitation settings, clinical translation of our findings is not difficult to envision.

Table 1.1. Subject Characteristics

| | Male (n = 10) | Female (n = 10) |
|---|---|---|
| Age (yrs) | 21.8 ± 0.67 | 20.1 ± 0.60 |
| Height (cm) | 179.8 ± 1.58 | 164.9 ± 2.99 |
| Mass (kg) | 75.0 ± 2.51 | 55.0 ± 2.40 |
| Thigh Skinfold Thickness (mm) | 16.1 ± 2.80 | 19.7 ± 2.28 |

All volunteers were considered healthy, free of any signs/symptoms of cardiovascular and/or metabolic disease. Data are expressed as means ± SEM, n = 20.

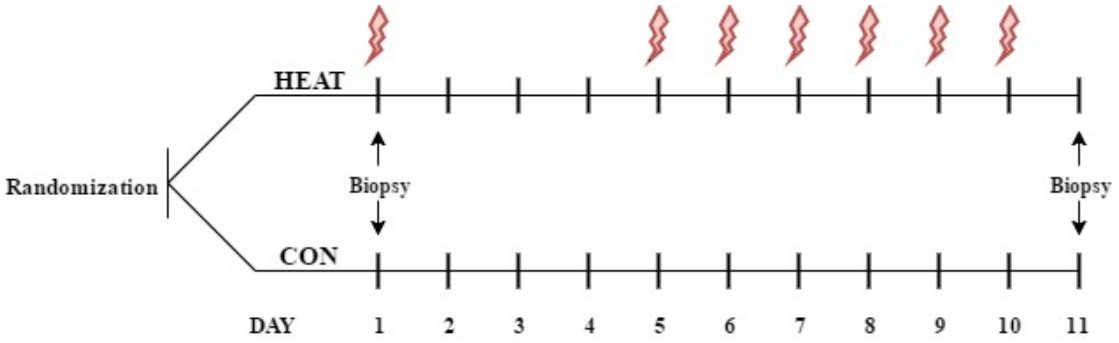


Figure 1.1. Study design. A leg of each volunteer was randomly selected to either receive pulsed shortwave diathermy treatments (HEAT) or serve as control (CON). Following randomization, heating was administered on days 1 and 5 to 10. Biopsies were taken from the vastus lateralis of both legs immediately following the 2-hour heating session on day 1 and again after the completion of the 6 day, 2 hours/day heating protocol on day 11.

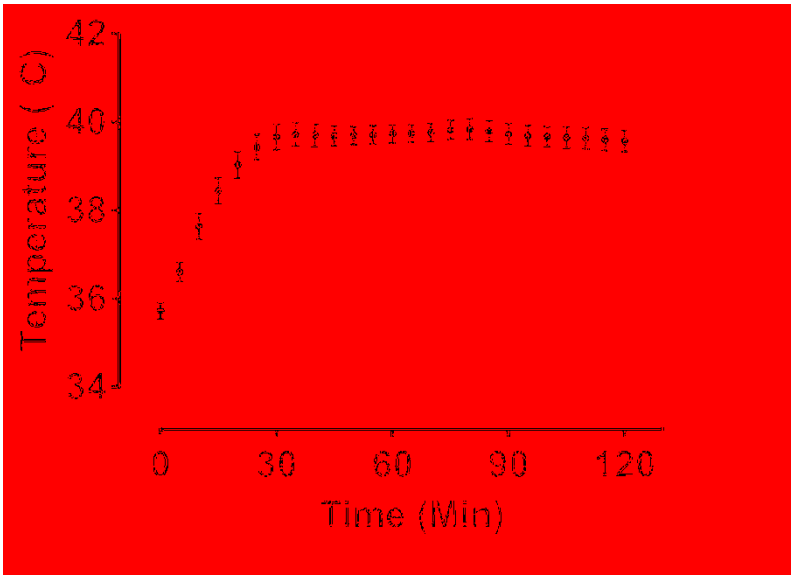

Figure 1.2. Muscle temperature. Intramuscular temperature was recorded during the first treatment with pulsed shortwave diathermy at a depth of ~3 to 3.5 cm. Data are expressed as means ± SEM, n = 20.

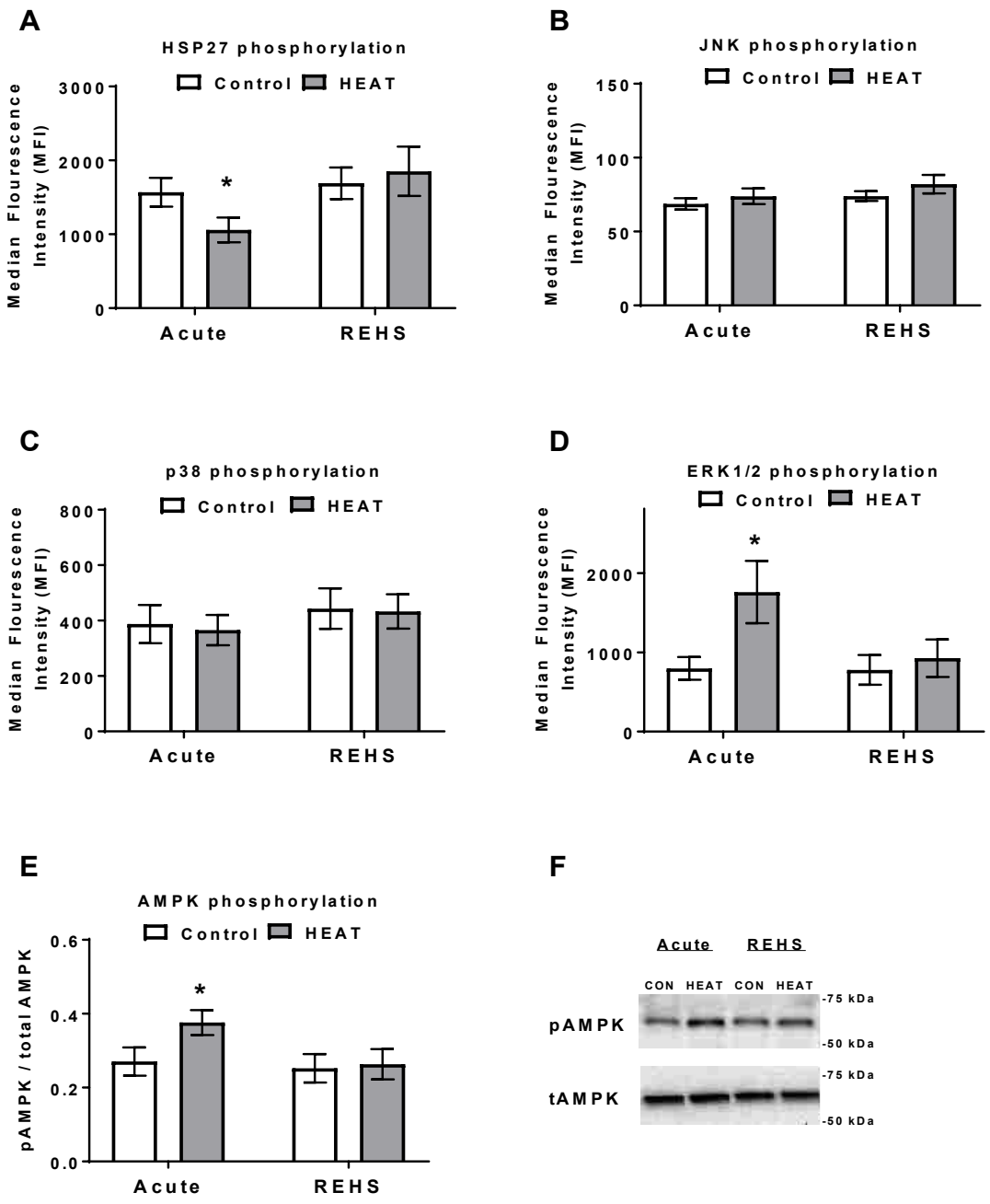


Figure 1.3. Cell signaling. Phosphorylation events immediately following a single, 2-hour heating session (Acute) and after 6 days of repeated exposure to heat stress (REHS). Magnetic-bead immunoassay panel results for differences in **(A)** HSP27 Phosphorylation **(B)** JNK phosphorylation, **(C)** p38 MAPK phosphorylation, and **(D)** ERK1/2 phosphorylation. **(E)** AMPK phosphorylation. **(F)** Representative protein immunoblot for pAMPK (CON = Control, HEAT = Heat assigned limbs). *$p < 0.05$, significant difference compared to control. Data are expressed as means ± SEM, n = 12-18.

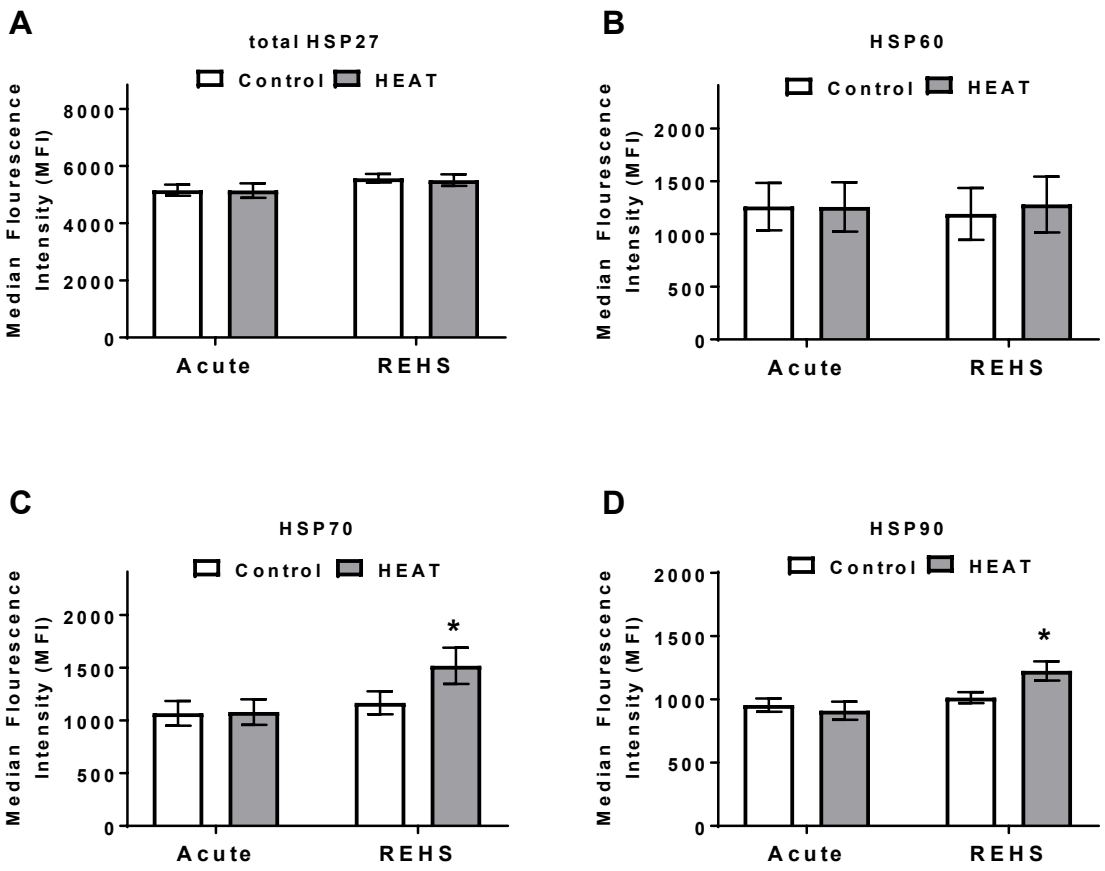


Figure 1.4. HSP expression. Measures taken following a single 2-hour heating session (Acute) and after 6 days of repeated exposure to heat stress (REHS). Magnetic-bead immunoassay panel results for **(A)** Total HSP27 expression **(B)** Total HSP60 expression **(C)** Total HSP70 expression **(D)** Total HSP90 expression. *$p < 0.05$, significant difference from baseline. Data are expressed as means ± SEM, n = 17-19.

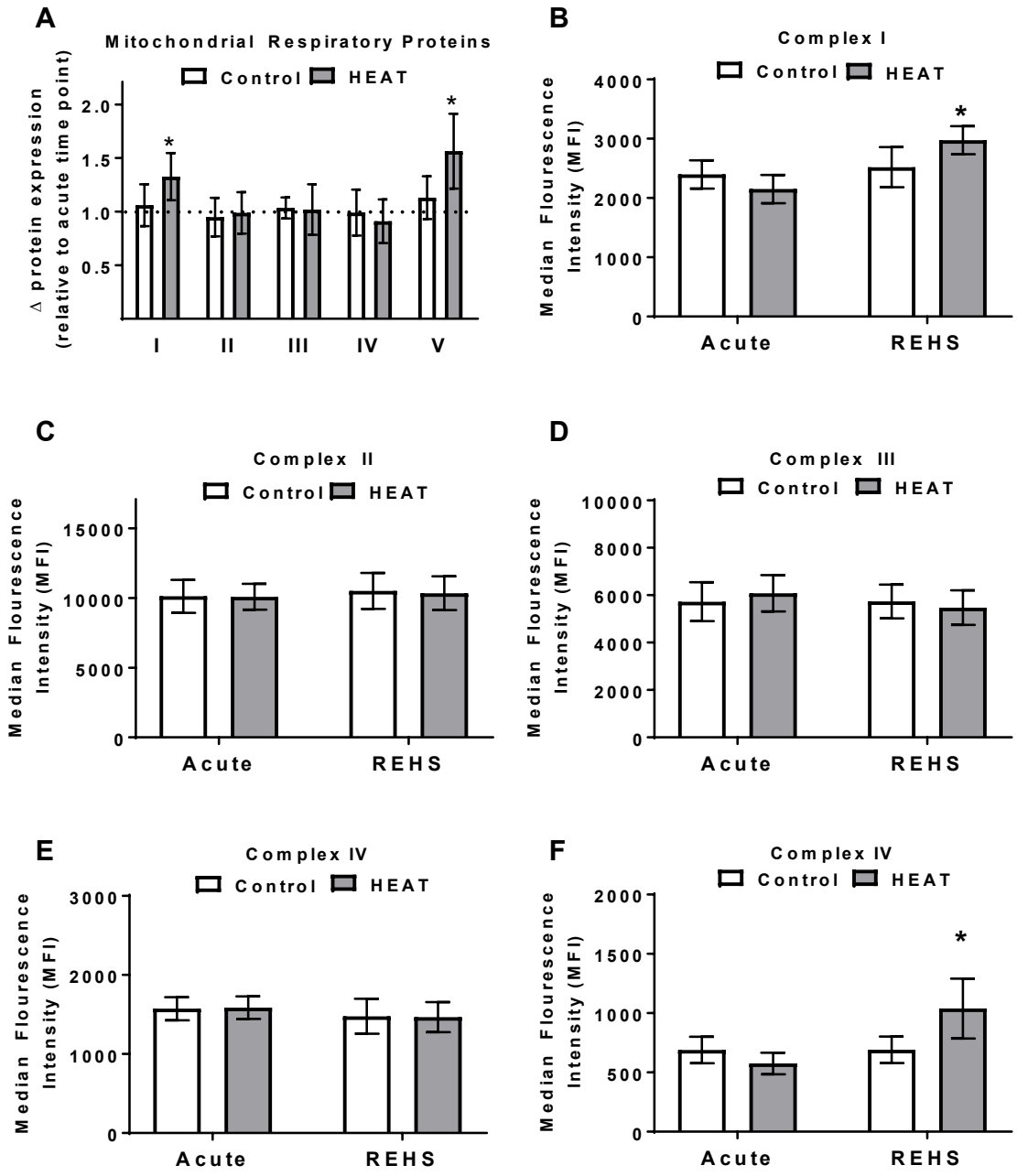


Figure 1.5. Mitochondrial respiratory protein expression. Magnetic-bead immunoassay panel results for changes in protein expression of the five mitochondrial respiratory proteins (I-NADH oxidase, II-succinate dehydrogenase, III-cytochrome c reductase, IV-cytochrome c oxidase, V-ATP synthase). **(A)** Summary of change observed between Acute and REHS time points. Protein expression immediately following an acute heat exposure (Acute) and after 6 days of repeated heat exposure (REHS) for **(B)** Complex I, **(C)** Complex II, **(D)** Complex III, **(E)** Complex IV, and **(F)** Complex V. *$p < 0.05$, significant increase following REHS. Data are expressed as means ± SEM, n = 15-18.

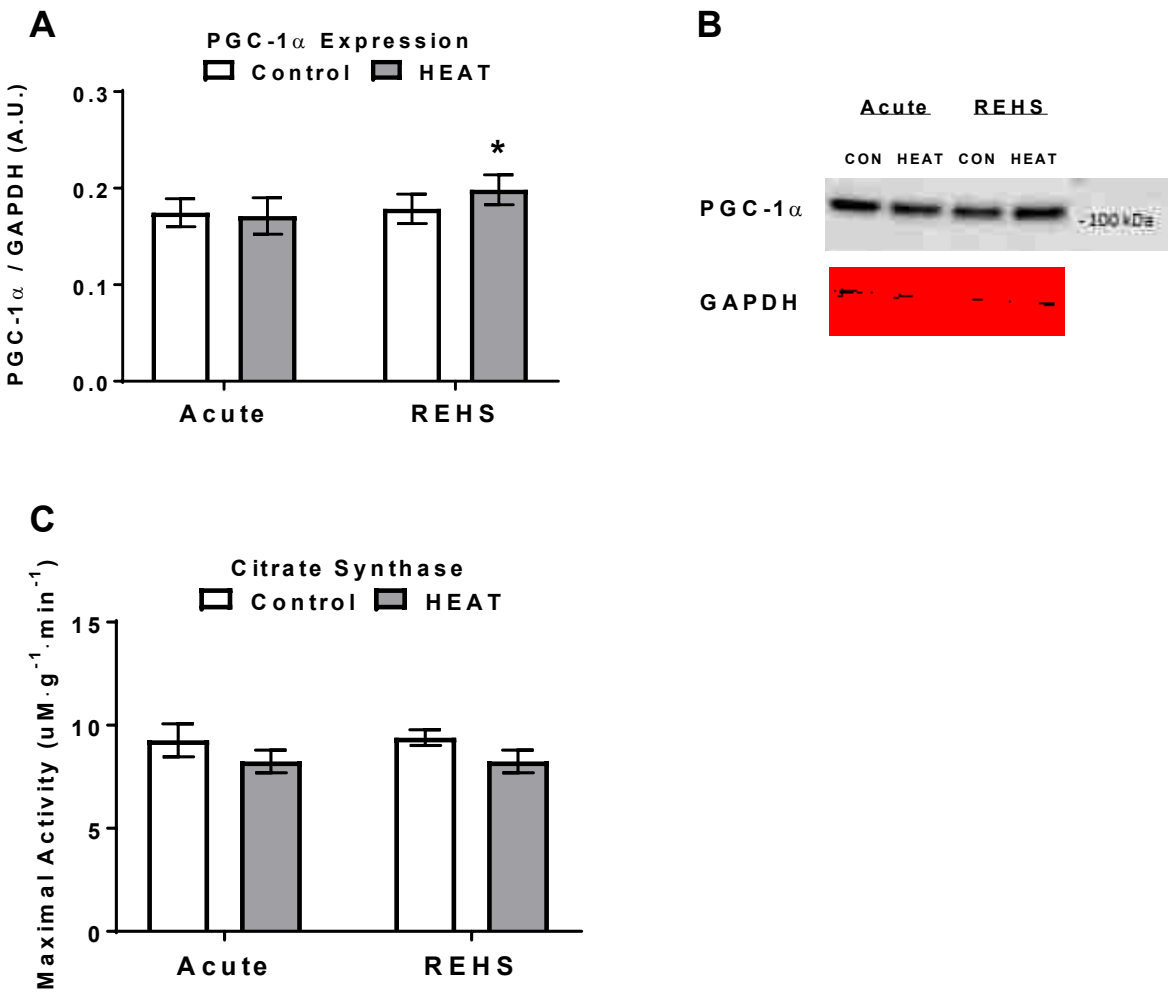


Figure 1.6. Additional markers of mitochondrial adaptation. **(A)** Expression of peroxisome proliferator-activated receptor gamma, coactivator-1 alpha (PGC-1α) relative to GAPDH **(B)** Representative protein immunoblot for PGC-1α and GAPDH **(C)** Maximal citrate synthase (CS) activity. *$p < 0.05$, significant increase following REHS. Data are expressed as means ± SEM, n = 14-18.

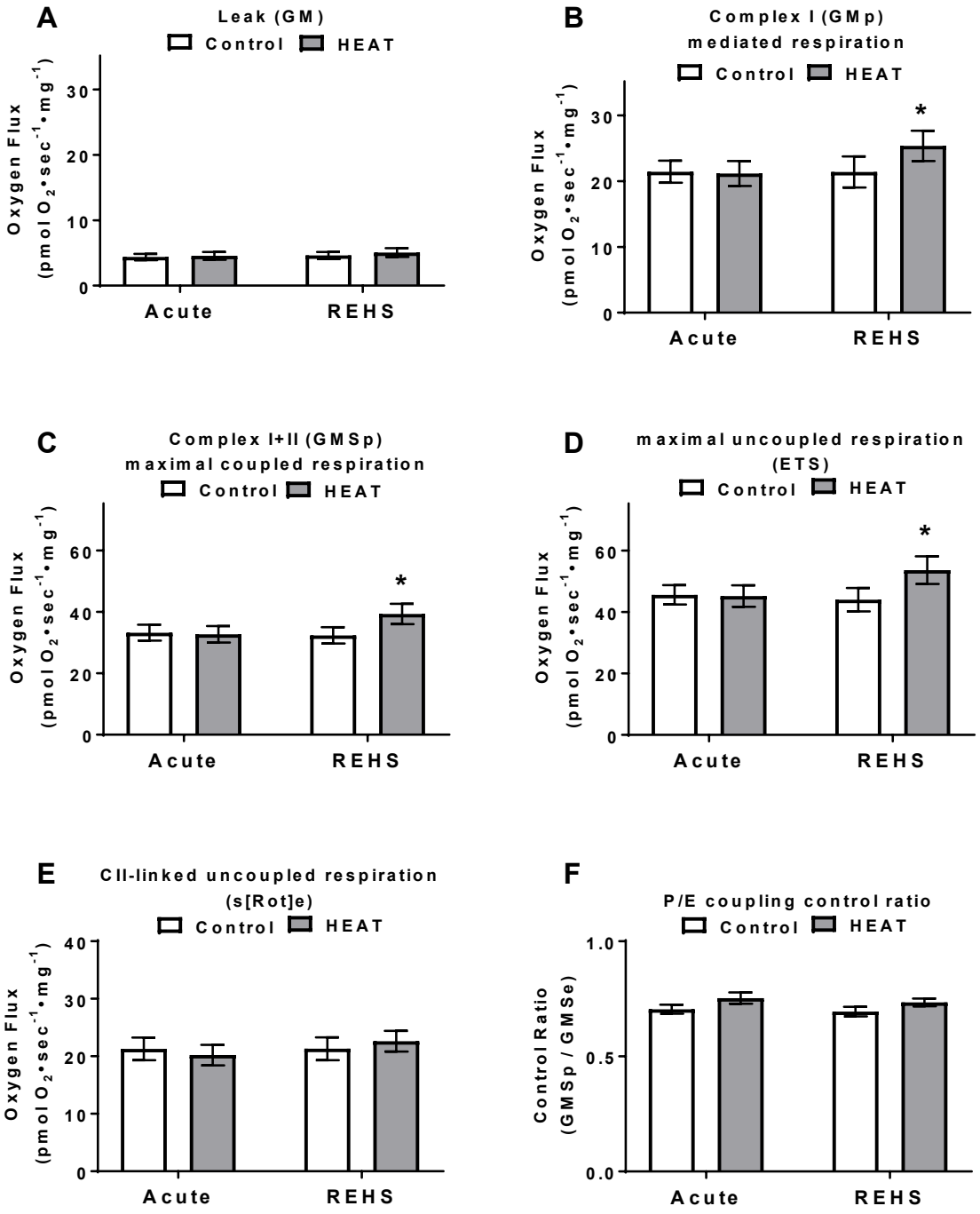


Figure 1.7. Mitochondrial respiratory capacity. Measures taken immediately following a single heat exposure (Acute) and again after 6 days of repeated exposure to heat stress (REHS). Oxygen flux for **(A)** Leak **(B)** Complex I-mediated respiration **(C)** Maximal coupled respiration **(D)** Maximal uncoupled respiration **(E)** Complex II- linked uncoupled respiration. **(F)** P/E coupling control ratio represents the limitation of respiratory capacity by the phosphorylation system. *$p < 0.05$, significant increase with REHS. Data are expressed as means ± SEM, n = 15-18.

Study 2

## Repeated Exposure to Heat Stress Protects Respiratory Capacity and Attenuates Muscle Atrophy in Human Skeletal Muscle Subjected to Immobilization


### Abstract

Skeletal muscle immobilization leads to atrophy, decreased metabolic health and substantial losses in function. Animal models suggest that heat stress is capable of providing protection against atrophy in skeletal muscle. This study investigated the effects of daily heat therapy on human skeletal muscle subjected to 10 days of immobilization. Muscle biopsies were collected from the vastus lateralis of 23 healthy volunteers (11 females, 12 males) before and after either 10 days of immobilization with a daily sham treatment (Imm), or with a targeted daily 2-hour heat treatment using pulsed shortwave diathermy (Imm + H). Diathermy increased intramuscular temperature 4.2 ± 0.29°C ($p < 0.0001$), with no change in the sham group. As a result, HSP70 and HSP90 increased ($p < 0.05$) following Imm + H (25 ± 6.6 and 20 ± 7.4%, respectively), but were unaltered ($p > 0.05$) with Imm only. Heat treatment prevented the immobilization-induced loss of coupled (−27 ± 5.2% vs. −8 ± 6.0%, $p = 0.0041$) and uncoupled (−25 ± 7.0% vs. −10 ± 3.9%, $p = 0.0302$) myofiber respiratory capacity. Likewise, heat treatment prevented the loss of proteins associated with all 5 mitochondrial respiratory complexes ($p < 0.05$). Furthermore, decreases in muscle cross-sectional area following Imm were greater than Imm + H at both the level of the whole-muscle (−7.6 ± 0.96% vs. −4.5 ± 1.09%, $p = 0.0374$) and myofiber (−10.8 ± 1.52% vs. −5.8 ± 1.49%, $p = 0.0322$). Our findings demonstrate that daily heat treatments, applied during 10 days of immobilization, prevent the loss of mitochondrial function and attenuate atrophy in human skeletal muscle.

Introduction

Skeletal muscle is a highly adaptable tissue that comprises approximately 40% of total body weight, while accounting for up to 90% of whole-body oxygen consumption and energy expenditure during exercise (5, 20). Furthermore, a substantial amount of research has shown that an adequate amount of muscle mass can prevent the development of several chronic diseases (e.g., type II diabetes and obesity) and is necessary to maintain work capacity throughout the lifespan (66, 86). While improvements in metabolic capacity, structure, and function of skeletal muscle occur in response to regular exercise training, these same characteristics are compromised during periods of physical inactivity or muscle disuse (33, 46).

The loss of skeletal muscle mass (atrophy) that accompanies disuse, results primarily from a decrease in intracellular protein synthesis combined with an increase in proteolytic activity (33). Interestingly, these processes appear to be affected by changes in muscle mitochondrial capacity, with evidence suggesting that the maintenance of mitochondria during periods of disuse protects skeletal muscle against atrophy (64). Remarkably, rodents with denervated muscle are protected against muscle atrophy following whole-body heat stress. The mechanism of protection appears to be tied to the observed increases in heat shock proteins (HSPs) and peroxisome proliferator-activated receptor gamma, coactivator-1 alpha (PGC-1α), which accompany the heat stress (75). These potential mechanisms of protection are supported by transgenic animal research that has shown significant reductions in muscle atrophy with the overexpression of either PGC-1α (68), HSP27 (16), or HSP70 (70).

Heat-induced protection against muscle atrophy has not yet been shown in human skeletal muscle. A significant barrier to testing this hypothesis in human muscle is finding a suitable modality to significantly increase intramuscular temperatures. There is some controversy

as to whether surface heating modalities (e.g., heating pad, hot water immersion, sauna) can raise muscle temperature sufficiently. For example, the use of superficial heating pads leads to robust temperature increases at a depth of 1 cm below the skin (~4°C), but only small increases (< 1°C) at depths approaching those of the deeper skeletal muscles (17). We have shown previously that pulsed shortwave diathermy results in significant increases in intramuscular temperature (~3 to 4°C), increasing both HSP and PGC-1α expression in human skeletal muscle (preliminary study). Thus, the aim of this study was to test whether daily heat stress would be capable of maintaining mitochondrial function and providing protection against muscle atrophy in human skeletal muscle subjected to 10 days of single-leg immobilization.

Methods

Twenty-four young adults (12 male, 12 female; 18 to 39 years) were recruited for this study. From these 24, one female participant was unable to complete the study due to personal commitments (not related to the study) that arose. Therefore, her data are not included in the analyses. Inclusion criteria included positive responses to the health screening questionnaire and participation in a regular exercise training program (≥3 hours/week). We included trained volunteers with the rationale that leg immobilization would present a larger disuse effect compared to their higher daily activity, as opposed to the little activity that would be expected within a sedentary group. Subject characteristics are available in Table 2.1. Exclusion criteria for subjects included known cardiac or peripheral vascular disease and/or a high body mass index (BMI > 25). The study protocol was approved by the Brigham Young University Institutional Review Board and conformed to the standards set by the Declaration of Helsinki.

The sample size estimate was calculated from data on previous reports of changes in muscle cross-sectional area (CSA) following short-term immobilization (78). The proposed

number of subjects was deemed appropriate to detect meaningful differences in muscle CSA with sufficient power (0.80) at alpha 0.05. This number of subjects also aligned with the number of subjects that had previously been used to show changes in gene expression and muscle CSA following short-term immobilization (13), sex-related differences in muscle atrophy (87), and therapeutic prevention of muscle atrophy (15).

**Design**. This study was a single-blinded, sham-controlled assessment on the effect of heat therapy on skeletal muscle subjected to immobilization. After providing written informed consent, the participants of the study reported to the laboratory to be fitted for the therapeutic knee brace (Bledsoe Revolution 3, Grand Prairie TX) and to receive instruction for the use of standard medical arm crutches. On the first scheduled day of the study, the left quadriceps muscle group of each participant was scanned using magnetic resonance imaging (MRI), after which muscle biopsies were collected. To allow adequate healing time for the muscle biopsy sites, we did not initiate the immobilization and heating protocol until 5 days following the first muscle biopsy.

For the immobilization protocol, the left leg of all participants was selected for immobilization and each participant was randomly assigned, in a counterbalanced fashion, to either the control (Imm; diathermy placed over the muscle but not emitting waves) or treatment (Imm + H; diathermy placed over muscle and emitting waves) group. The counterbalanced assignment of participants to these groups was done to ensure the balance of BMI and self-reported participation in exercise training between groups (characteristics are provided in Table 2). All participants reported to the lab for 2 hours per day over the 10 consecutive days of immobilization to receive their heating or sham treatment. We did not inform individuals which group they belonged to (heat vs sham). As the subjects were unfamiliar with the sensations

associated with diathermy treatment, we believed that the contact of the heating drum on the skin for 2 hours would provide a superficial sensation of warming without resulting in deep tissue heating. For confirmation of intramuscular temperature during treatments, a small sterile temperature microprobe was inserted approximately 3.5 cm into the muscle during the first treatment session in order to confirm intramuscular temperatures. The microprobe was inserted perpendicular to the muscle using a small 20-gauge sterile catheter. Additionally, all subjects reported their sensations of heat during the first treatment visit using a 10 cm visual analog scale with sensations ranging from 'no warmth' to 'extremely hot.' The area of heating was marked with a black marker to ensure proper placement of the diathermy drum for all subsequent treatments.

Participants reported to the laboratory 24 hours after their last heating session for the final MRI scan and muscle biopsies, according to the procedures used for the baseline measures (Figure 2.1). The immobilization brace was removed and participants were able to reload their leg following these final measures.

**Magnetic resonance imaging.** Before each MRI scan, volunteers completed a safety survey sheet to confirm that it was safe for them to complete the scanning procedure. For each scan (pre and post), volunteers lay supine in a 3.0 Tesla MRI scanner (Siemens Healthineers, Erlangen DEU). The leg was aligned with the toes pointed upward to ensure consistency between measures. A stock Siemens 2-D multislice gradient-recalled echo (GRE) MRI pulse sequence was used for this study. The images were taken in slices, every 5 mm, resulting in a total sequence time of approximately 2 minutes. This provided cross-sectional images of the thigh from the base of the femur (distal condyles) up to the groin. In addition, a thin silicon mold, the size of the diathermy heating drum, was placed over the area marked for heating. This

area was on the lower one-half to one-third portion of the vastus lateralis, depending on the size of the volunteer. Thus, slices from the treatment area could be confirmed and images compared before and after the immobilization period.

**Muscle biopsies.** Percutaneous needle biopsies were taken from the vastus lateralis muscles of the left leg for assessment of mitochondrial respiratory capacity, fiber cross-section area, and protein analyses. Biopsies were taken on the first visit (pre) and upon conclusion of the immobilization protocol (post). A small area on the skin over the vastus lateralis was shaved and then cleaned with the antiseptic chlorhexidine. After sterilization, injection of a local anesthesia (1% lidocaine with epinephrine) was used to numb the area. After the participant reported no sensation in the area, a small incision was made into the skin and fascia and the biopsy needle was inserted into the muscle. Using manual suction, approximately 75 to 150 mg of tissue was withdrawn. Muscle samples were separated from any fatty tissue and divided into 25 to 50 mg portions. A small 5 to 10 mg portion was immediately placed in a cell buffer solution for analysis of respiratory capacity. Other portions of tissue designated for protein analysis were frozen in liquid nitrogen, while portions designated for immunohistochemistry were mounted on a cork with tragacanth gum and frozen in isopentane cooled in liquid nitrogen. All frozen samples were stored at −80°C for analysis following completion of the study. Follow-up biopsies that were performed on the same leg following immobilization were taken approximately 5 cm proximal to the first incision site to minimize potential confounding effects from previous biopsies.

**Mitochondrial respiration.** Measurements of skeletal muscle mitochondrial respiration were performed on permeabilized fibers using a Clarke oxygen electrode high-resolution respirometer (Oxygraph O2k, Oroboros Instruments, Innsbruck AUT). Using fine-tipped forceps, fibers were gently separated (teased) from one another to maximize surface area of the fiber

bundle with only small portions connected to ensure that fibers were not disconnected or lost during permeabilization. Following teasing, fibers were carefully dried on fresh filter paper and weighed before being placed in ice-cold *buffer X* (60 mM K-MES; 35 mM KCl; 7.23 mM $K_2$EGTA; 2.77 mM Ca$K_2$EGTA; 20 mM imidazole; 0.5 mM DTT; 20 mM taurine; 5.7 mM ATP; 15 mM PCr; and 6.56 mM $MgCl_2$). The measurement of sample dry weight allowed respiratory measures to be normalized between runs and accounted for potential differences in chamber loading. Fibers (3 to 6 mg) were then permeabilized with the addition of saponin to a final concentration of 50 µg/ml. To assess mitochondrial respiratory capacity, we followed a standard substrate-uncoupler-inhibition-titration (SUIT) protocol, allowing us to assess individual components of the respiratory chain (25). All respiratory experiments were carried out in MiRO5 (110 mM sucrose; 60 mM potassium lactobionate; 2 mM magnesium Chloride; 20 mM taurine; 10 mM potassium phosphate; 0.5 mM EGTA; 20 mM HEPES; and 1 g/L BSA) at 25°C with spinning at 750 rpm. Oxygen concentrations were maintained between 500 and 200 µM throughout each experiment.

The SUIT protocol began with the addition of glutamate (10 mM) and malate (2 mM). After allowing for steady-state reading of oxygen uptake in the presence of glutamate and malate (leak), ADP (2.5 mM) was added to drive respiration through Complex I ($P_I$; CI). Following the measurement of CI-mediated respiration, cytochrome c (10 µM) was added to confirm integrity of the outer mitochondrial membrane. Stimulation of respiration by added cytochrome c would indicate injury to the membrane. We did not observe a positive cytochrome c response in any of our samples permeabilized with saponin. Following confirmation of intact mitochondrial membranes, succinate (10 mM) was added to stimulate respiration through Complex II ($P_{I+II}$; CII). Thus, we were able to measure maximal coupled respiration (OXPHOS) as both CI and CII

were contributing to the total oxygen flux. Maximal uncoupled respiratory capacity (E; ETS) was then assessed with the addition of the uncoupler FCCP (2 to 3 steps of 0.125 µM FCCP). The response following the addition of FCCP demonstrates the limits of the phosphorylation system observed from OXPHOS. After measuring ETS, rotenone (0.5 µM) was added to inhibit CI, so that only CII could be contributing to the uncoupled respiratory processes. Finally, residual oxygen consumption (ROX) was measured following the addition of Antimycin A (2.5 µM) to inhibit Complex III. ROX was subtracted from oxygen flux as a baseline for all respiratory states.

**Muscle protein measures.** Muscle tissue was homogenized in chilled homogenization buffer (50 mM Tris-HCl, pH 7.4; 250 mM mannitol; 50 mM NaF; 5 mM Sodium Pyrophosphate; 1 mM EDTA; 1 mM EGTA; 1% Triton X-100; 50 mM β-glycerophosphate), with added protease inhibitors (1% Halt™ Protease Inhibitor Cocktail, Thermo Fisher Scientific, Waltham MA), at a volume of 10 µl per 1 mg tissue. Homogenates were centrifuged at 600*g* for 10 minutes at 4°C, and the supernatants were transferred to clean tubes and stored at −80ºC. Protein concentration was determined using a Pierce™ Bicinchoninic Acid (BCA) Kit (Thermo Fisher Scientific, Waltham MA) and spectrophotometer (Victor3™, Perkin Elmer, Waltham MA), according to the manufacturer's specifications. Samples were diluted with 2x loading buffer (125 mM Tris, pH 6.8; 4% SDS; 20% glycerol; 5% BME; 0.01% bromophenol blue) to a concentration of 1 µg/µl (20 µg total) and ran on a 4 to 15% graded SDS-polyacrylamide gel (Bio-Rad, Hercules CA) at 200 V for 50 minutes at room temperature. Both samples from each subject were run on the same gel to avoid any variability between gels. Following electrophoresis, proteins were transferred to a PVDF membrane at 100 V for 60 min at 4ºC. Following transfer, membranes were immersed in a Ponceau Red staining solution for 1 minute,

rinsed in $dH_2O$ for 5 minutes, and imaged for total protein. Membranes were then blocked in 5% milk diluted in tris-buffered saline with Tween (TBST) for 60 minutes at room temperature. Following blocking, membranes were incubated in primary antibodies diluted in 5% bovine serum albumin (BSA) in TBST overnight at 4ºC. The primary antibodies used in this study were for HSP70 (1:1000, Enzo Life Sciences #ADI-SPA-811-D, Farmingdale NY), HSP90 (1:3000, Enzo Life Sciences #ADI-SPA-831/050, Farmingdale NY), PGC-1α (1:1000; EMD Millipore #AB3242, Burlington MA), MAFbx (1:1000, Santa Cruz Biotech #sc-166806, Dallas TX), Murf1 (1:3000, Abcam #ab96857, Cambridge UK), and Total Oxphos Human Cocktail (1:1000, Abcam #ab110411, Cambridge UK). The Total Oxphos Human Cocktail consisted of 5 antibodies, 1 each against Complex I subunit NDUFB8 (#ab110242), Complex II subunit 30 kDa (#ab14714), Complex III subunit Core 2 (#ab14745), Complex IV subunit II (#ab110258), and ATP synthase subunit alpha (#ab14748). Following the primary antibody incubation, each membrane was washed in TBST and probed with either anti-mouse or anti-rabbit secondary antibodies (1:5,000; Santa Cruz Biotech). The bands of interest were then exposed through chemiluminescence (ECL) and imaged using ChemiDoc XRS (Bio-Rad, Hercules CA) CCD high-resolution, high-sensitivity technology. Data were normalized to total protein (Ponceau Red) to account for potential variations in loading.

**Muscle fiber morphology.** Tissue sections were immunostained for dystrophin, myosin heavy chain I, and DAPI. Dystrophin allowed visualization of the muscle fiber membranes to increase accuracy of CSA measures, while myosin heavy chain staining was used to differentiate between Type I and Type II fibers. For the determination of CSA, 8 μm transverse sections were cut at −25°C, placed on slides, and fixed in 2% paraformaldehyde. Following fixation and rinsing, samples were blocked for 1 hour at room temperature in a PBS blocking solution (5%

goat serum and 2% BSA). Samples were then incubated overnight at 4°C in a covered, humidified chamber with primary antibodies for dystrophin (1:100, Abcam #ab15277 rabbit host, Cambridge UK) and myosin heavy chain I (1:100, DSHB, #BA-D5 mouse host, Iowa City IA). Following incubation with primary antibodies, samples were rinsed in PBS and incubated for 60 minutes at 37°C in a covered, humidified chamber in the secondary solution containing DAPI (1:1000, Thermo Fisher Scientific #D1306, Waltham MA), and secondary antibodies (Rhodamine Red anti-mouse, 1:100, Jackson IR, and Alexa Fluor 488 anti-rabbit, 1:100, Jackson IR, West Grove PA, respectively). Samples were then mounted in fluoroshield mounting medium before the application of a cover slip. Imaging was done using an Olympus IX73 microscope and Olympus XM10 camera (Olympus Corp, Tokyo JPN). Images were taken at 10 and 20X magnifications. Approximately 80 to 100 fibers were traced for each Type (I and II) in order to calculate mean myofiber CSA before and after immobilization.

**Data analysis.** A mixed models analysis of variance (ANOVA) was used to examine the effects of time (pre vs. post) and group (Imm vs. Imm + H) on our dependent variables (mitochondrial respiration, protein content, CSA). In the case of a significant [time × group] interaction, individual comparisons were made using student *t*-tests with Bonferroni corrections for multiple comparisons. JMP® Pro 13.0.0 (©SAS Institute, 2016) statistical software was used for all statistical analyses with alpha set a priori at 0.05. Data are presented as Mean ± SEM.

Results

**Subject characteristics.** Twenty-three young adults (12 male, 11 female; 18 to 39 years) completed this study. Descriptive data for each of the 2 groups (Imm and Imm + H), further divided into sex categories, are provided in Table 2.1. There were no statistical differences observed between groups for age, height, weight, body mass index (BMI), or self-reported

weekly exercise volume. However, the female subjects displayed significantly lower measures of body height ($p < 0.0001$) and weight ($p = 0.0010$) compared to their male counterparts. As both height and weight were lower in females on average, this resulted in similar BMI values between sexes ($p = 0.5819$). Furthermore, the changes in our dependent variables did not display any significant sex effects, so the data were pooled (males and females) within groups.

**Intramuscular temperature and HSP expression**. Diathermy treatment resulted in a significant increase ($4.2 \pm 0.29$°C, $p < 0.0001$) in intramuscular temperature, while there was no change observed in the sham group during the 2-hour sham treatment (Figure 2.2). Reported sensations of warmth from the 10 cm visual analog scale increased during the 2-hour diathermy treatment session in both groups ($p < 0.0001$ and $p = 0.004$, respectively). Additionally, the heating group (Imm + H) reported higher levels of warmth than the sham (Imm) group ($3.6 \pm 0.16$ vs. $1.7 \pm 0.15$ cm, respectively, $p < 0.0001$; Figure 9). Following the 10-day treatment period, the Imm + H group displayed increases in HSP70 ($25 \pm 5.2\%$, $p = 0.0002$) and HSP90 ($20 \pm 7.4\%$, $p = 0.0059$) protein expression. With Imm only, HSP70 and HSP90 were unchanged following the 10-day immobilization period ($p = 0.5024$ and $p = 0.0798$, respectively; Figure 2.2).

**Mitochondrial respiratory capacity**. In response to immobilization, mitochondrial respiratory dynamics were significantly altered (Figure 2.3). The Imm group displayed increased leak (GM; $5.39 \pm 0.49$ vs. $7.69 \pm 0.97$ $pmolO_2 \cdot sec^{-1} \cdot mg^{-1}$, $p = 0.0136$). In the absence of ADP, this increased leak with Imm suggests greater intrinsic uncoupled respiration when oxygen flux is elevated to compensate for the proton leak as opposed to active phosphorylation of ADP to ATP. In addition, Imm resulted in decreased respiratory capacity when measured as CI-mediated (GMp; $32.6 \pm 2.92$ vs. $21.0 \pm 2.00$ $pmolO_2 \cdot sec^{-1} \cdot mg^{-1}$, $p = 0.0003$), maximal coupled (GMSp;

51.3 ± 3.62 vs. 36.3 ± 2.45 pmol$O_2$·$sec^{-1}$·$mg^{-1}$, p = 0.0001), maximal uncoupled (GMSe; 65.5 ± 5.84 vs. 46.8 ± 3.65 pmol$O_2$·$sec^{-1}$·$mg^{-1}$, p < 0.0001), and CII-mediated uncoupled (S[Rot]e; 28.4 ± 2.55 vs. 21.4 ± 1.50 pmol$O_2$·$sec^{-1}$·$mg^{-1}$, p = 0.0001) respiration. However, with daily heat therapy (Imm + H), mitochondrial respiratory dynamics were maintained following the immobilization protocol, as there were no changes in GM (p = 0.5184), GMp (p = 0.5116), GMSp (p = 0.6553), GMSe (p = 0.0884), or S[Rot]e (p = 0.0655). Furthermore, with Imm only, these alterations resulted in decreased OXPHOS coupling efficiency (0.88 ± 0.017 vs. 0.77 ± 0.038, p = 0.0003) and ETS coupling efficiency (0.91 ± 0.016 vs. 0.83 ± 0.024, p < 0.0001), while neither OXPHOS or ETS coupling efficiency was changed following Imm + H (p = 0.8723 and p = 0.7407, respectively). We observed no changes in the OXPHOS control ratio (P/E coupling control ratio) within either group (Figure 2.3).

**Mitochondrial respiratory proteins**. In conjunction with decreased respiratory capacity, Imm resulted in decreases in the expression of proteins for all 5 of the respiratory protein complexes. Specifically, we observed decreases in Complex I subunit NDUFB8 (−10 ± 2.3%, p = 0.0056), Complex II subunit 30 kDa (−15 ± 3.5%, p = 0.0043), Complex III subunit Core 2 (−8 ± 2.3%, p = 0.0133), Complex IV subunit II (−22 ± 8.6%, p = 0.0106), and ATP synthase subunit alpha (−9 ± 1.5%, p = 0.0020). However, Imm + H prevented the decrease in protein expression (Figure 2.4). Moreover, we observed decreases in the expression of PGC-1α with Imm (0.54 ± 0.039 vs. 0.50 ± 0.037 AU, p = 0.0284). Conversely, with Imm + H, PGC-1α expression was increased following the 10-day immobilization period (0.49 ± 0.056 vs. 0.54 ± 0.064 AU, p = 0.0337; Figure 2.4).

**Muscle cross-sectional area**. Whole-muscle CSA decreased 7.3% with Imm (2304 ± 197 vs. 2143 ± 196 $mm^2$, p < 0.0001). The decrease in vastus lateralis CSA was significantly

larger ($p = 0.0256$) than the 4.5% decrease observed with Imm + H (2089 ± 149 vs. 1995 ± 150 $mm^2$, $p = 0.0010$).

Similarly, myofiber CSA decreased by 10.8% with Imm (5631 ± 445 vs. 5035 ± 400, $p < 0.0001$). This decrease was significantly larger ($p = 0.0359$) than the 5.8% decrease following Imm + H (6120 ± 434 vs. 5766 ± 441, $p = 0.0008$). In addition, while Type I fibers were significantly smaller than Type II fibers ($p = 0.0051$), fiber type did not demonstrate an interactive ($p = 0.9340$) effect on changes in CSA between groups over time. Thus, the degree of atrophy appeared to be independent of fiber type (Figure 2.5).

**E3 ubiquitin ligases**. Among the most studied ubiquitin ligases, we explored whether heating would affect changes in either MAFbx and Murf1. We did not observe any main effects of time ($p = 0.3665$ and $p = 0.4214$, respectively) or group ($p = 0.2384$ and $p = 0.0774$) on these 2 proteolytic markers. Furthermore, we were unable to identify an interactive (time x group) effect ($p = 0.1014$ and $p = 0.3888$, respectively) on these markers, suggesting that neither the immobilization or heating protocols affected changes in their expression at the 2 time points used in this study (Figure 2.6).

## Discussion

This study provides the first evidence that deep-tissue heating in human skeletal muscle subjected to immobilization is capable of maintaining mitochondrial function and attenuating muscle atrophy. These findings are consistent with previous explorations using whole-body heat stress as a means to combat disuse atrophy in rodents. For example, Naito et al. (55) showed that a single, 60-minute exposure to heat in an environmental chamber could protect against short-term atrophy of rat skeletal muscle. In addition, Tamura et al. (75) provided evidence that daily, 30-minute exposure to similar environmental thermal stress (40°C) could not only attenuate

muscle atrophy, but also suppress mitochondrial clearance and maintain oxidative capacity in rat skeletal muscle. Our findings in humans add to a growing body of literature that suggests heat treatment as a potential countermeasure for the metabolic and functional consequences that accompany muscle disuse.

We observed significant alterations in mitochondrial respiratory capacity with Imm. First, we observed a significant increase in leak respiration, which, in the absence of ADP, suggests that oxygen flux is increased through intrinsic uncoupling. While we did not measure changes in uncoupling proteins in our study, research in rodents shows that skeletal muscle denervation results in large increases in uncoupling protein mRNA expression (12). It was proposed that increases in uncoupling proteins under such conditions might facilitate tissue-specific temperature homeostasis as a result of the associated metabolic perturbations. Second, with Imm we observed significant decreases in both coupled and uncoupled respiratory capacity that were accompanied by decreased expression of proteins for all 5 mitochondrial respiratory complexes. These findings reinforce previous observations that 2 weeks of leg immobilization results in substantial losses of respiratory proteins and mitochondrial respiratory capacity in both the young and elderly (26). Loss of mitochondrial function has been widely implicated in the pathogenesis of skeletal muscle atrophy. In mice, interventions targeting the improvement of mitochondrial function, including repeated heat stress, prior to or during disuse have been effective at reducing the extent of muscle atrophy (49, 53, 75). Further, transcriptomic and proteomic studies have demonstrated profound decreases in metabolic- and mitochondrial-related proteins, which precede human muscle atrophy during periods of disuse (7). Thus, the preservation of mitochondrial function observed here appears to be an important mechanism for heat-induced muscle sparing. Remarkably, though, we show that daily muscle heating is capable

of preventing the loss of the respiratory proteins and preserving mitochondrial respiratory capacity.

We have previously shown that 6 consecutive days of heating increases intramuscular PGC-1α expression in human skeletal muscle. Given that overexpression of PGC-1α in rodents results in protection against disuse atrophy (6, 68), increases in PGC-1α may be an underlying mechanism to explain the metabolic and muscle-sparing effects of heat therapy. Thus, the decreased respiratory capacity observed with Imm may, in part, be explained by the concomitant decrease in PGC-1α expression. While Imm resulted in a significant decrease in PGC-1α expression, our heating protocol not only prevented the decrease, but in fact increased PGC-1α expression, potentially driving beneficial mitochondrial adaptations in the face of the disuse stimulus.

In addition to maintaining mitochondrial function, muscle atrophy was reduced by 37% with daily heat therapy. It is likely that this muscle-sparing effect of heat therapy can be attributed not only to the beneficial metabolic adaptations observed (increased PGC-1α and preserved mitochondrial function), but also to increased expression of the heat shock proteins (HSPs). In this study, both HSP70 and HSP90 were significantly increased following Imm + H. When overexpressed in rodent skeletal muscle, HSP70 has been shown to completely abolish skeletal muscle atrophy caused by immobilization (70). To further explore how heat stress might attenuate skeletal muscle atrophy in our study, we measured the expression of the E3 ubiquitin ligases (MAFbx and Murf1) that were also modified with HSP70 (70) and PGC-1α (68) overexpression in animals.

Contrary to our hypothesis that heating would attenuate immobilization-induced increases in these ligases, we were unable to detect any differences in MAFbx or Murf1

expression resulting from immobilization itself and/or heating. These results add to the growing body of evidence suggesting that the large increases in ubiquitin ligases observed in animal studies may not be apparent during human muscle disuse. While large increases in both mRNA and protein expression of MAFbx have been reported in patients suffering from amyotrophic lateral sclerosis (41), the time course for these proteins during disuse interventions in humans is much less understood and potentially more complicated. For example, short-term immobilization of 48 hours (1, 24, 82), 11 days (11), and 14 days (35) have resulted in transient increases in mRNA expression of MAFbx/Murf1, but these increases often do not necessarily manifest themselves in alterations in protein expression at these same time points. Furthermore, while Glover et al. (24) observed a transient (48 hours) increase in ubiquinated proteins, there was no increase in intracellular ubiquitination at 14 days of immobilization. This led the authors to suggest that perhaps single-leg immobilization in humans does not represent a catabolic model sufficient to observe measurable changes in static proteolytic enzyme levels or actin fragmentation (24). It is also important to note that we were unable find literature confirming the specificity of our antibodies to MAFbx/Murf1. Thus, the most likely explanations for our lack of any observable changes in MAFbx/Murf1 expression with our immobilization protocol is that the disuse stimulus was not extreme enough to drive measurable changes in the expression of these particular ubiquitin ligases and/or our antibodies were not specific to the proteins of interest.

While we were unable to observe changes in the ubiquitin ligases associated with muscle breakdown, the heat-induced protection against muscle atrophy observed in our study may have resulted from changes in muscle protein synthesis rates. While protein synthesis rates are reduced markedly with short-term immobilization in humans (21, 23), our heating protocol may have attenuated the reduction in protein synthesis. This is supported by previous research

showing that HSP70 assists in protein translation as it assists in nascent polypeptide folding (39, 56, 79).

While our focus was on specific changes measurable from within the muscle itself, we cannot determine the extent to which other tissues/systems in the area may have been influenced by our heating protocol. For example, a majority of the extracellular matrix surrounding skeletal muscle is produced by fibroblasts that reside in the interstitial space between muscle fibers (10). When subjected to heat shock, fibroblasts produce a variety of factors including HSPs (42, 59) and fibroblast growth factor-1 (34). Also, among the most robust physiological responses to diathermy is an increase in blood flow brought about by local hyperthermia (69, 85). Such circulatory responses to hyperthermia may increase delivery of systemic nutrients (22), alter fluid distribution among tissue compartments (45), and impact the release of shear-induced endothelial derived factors (19). Although we applied a localized heat stress, our tissue of interest (skeletal muscle) was not entirely isolated from other cell types and/or tissues, as it was performed in vivo. Therefore, while heat stress may directly affect skeletal muscle cells (44), the effects of hyperthermia on other cells/tissues/systems should not be overlooked when exploring potential mechanisms.

In conclusion, we show that heat therapy, applied for 2 hours daily during 10 days of immobilization, prevents loss of mitochondrial function and attenuates atrophy in human skeletal muscle. The results of the study have clear and potentially far-reaching clinical implications. While exercise interventions remain the most effective strategy to maintain or even increase respiratory capacity and/or muscle size, many patients for whom exercise would be most beneficial are either unable to exercise (i.e., postsurgery immobilization, on bed rest) or have very low tolerance for exercise (i.e., aged, obese, diseased populations). In these populations,

heat therapy may serve as an alternative or adjunct therapy to maintain skeletal muscle metabolic function and size.

Table 2.1. Subject Characteristics

| Group | Sex | Age, yrs | Ex, hours | Height, cm | Weight, kg | BMI, kg/m$^2$ |
|---|---|---|---|---|---|---|
| CON | Male n = 6 | 21.8 (0.67) | 4.5 (0.67) | 177 (2.23) | 72.0 (2.58) | 23 (1.03) |
| | Female n = 5 | 20.8 (1.07) | 5.1 (1.02) | 163 (4.00)* | 59.6 (3.85)* | 22.3 (1.11) |
| | **Group** n = 11 | **21.4 (0.58)** | **4.8 (0.57)** | **171 (2.97)** | **66.4 (2.89)** | **22.7 (0.73)** |
| HEAT | Male n = 6 | 22.8 (1.19) | 4.6 (0.42) | 182 (2.47) | 76.7 (4.89) | 23.1 (1.29) |
| | Female n = 6 | 21.2 (0.83) | 5.2 (0.60) | 164 (2.72)* | 60.2 (3.02)* | 22.5 (1.35) |
| | **Group** n = 12 | **22 (0.74)** | **4.9 (0.36)** | **172.8 (3.24)** | **68.4 (3.70)** | **22.8 (0.90)** |

There were no group differences observed in the descriptive variables associated with this study.
*$p < 0.05$, significantly lower height and weight observed in female volunteers compared to males.
Ex = self-reported weekly exercise time (hours). Data are Mean (SEM).

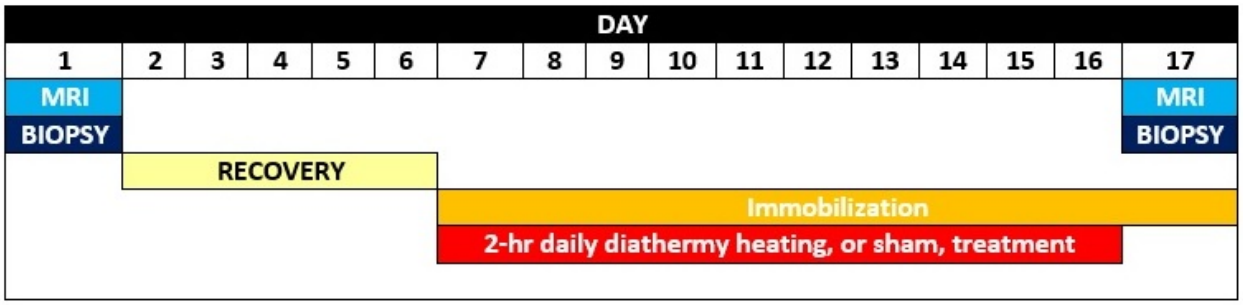


Figure 2.1. Study design. On days 1 and 17, volunteers reported to the laboratory for an MRI scan and muscle biopsy. Following a brief (5 day) recovery window after the baseline sample collection, immobilization and treatments (diathermy or sham) began on day 7 and ended following the collection of tissue on day 17.

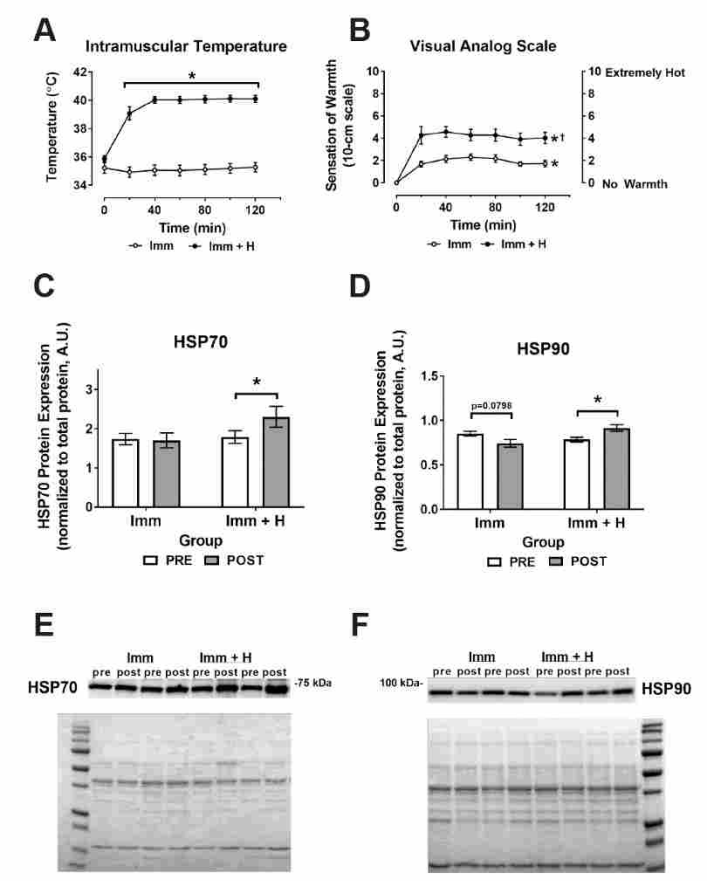


Figure 2.2. HSP and temperature response. A single, 2 hour diathermy treatment (Imm + H) resulted in elevated **(A)** intramuscular temperature, and **(B)** sensations of warmth compared to control (Imm). Following the 10-day immobilization period, **(C)** HSP70 and **(D)** HSP90 were significantly increased with Imm + H. Representative blots and Ponceau Red stains for **(E)** HSP70 and **(F)** HSP90. *$p < 0.05$, significant increase from baseline (pre). †$p < 0.05$, significantly different sensation of warmth between groups. Data are mean ± SEM, n = 18 to 23.

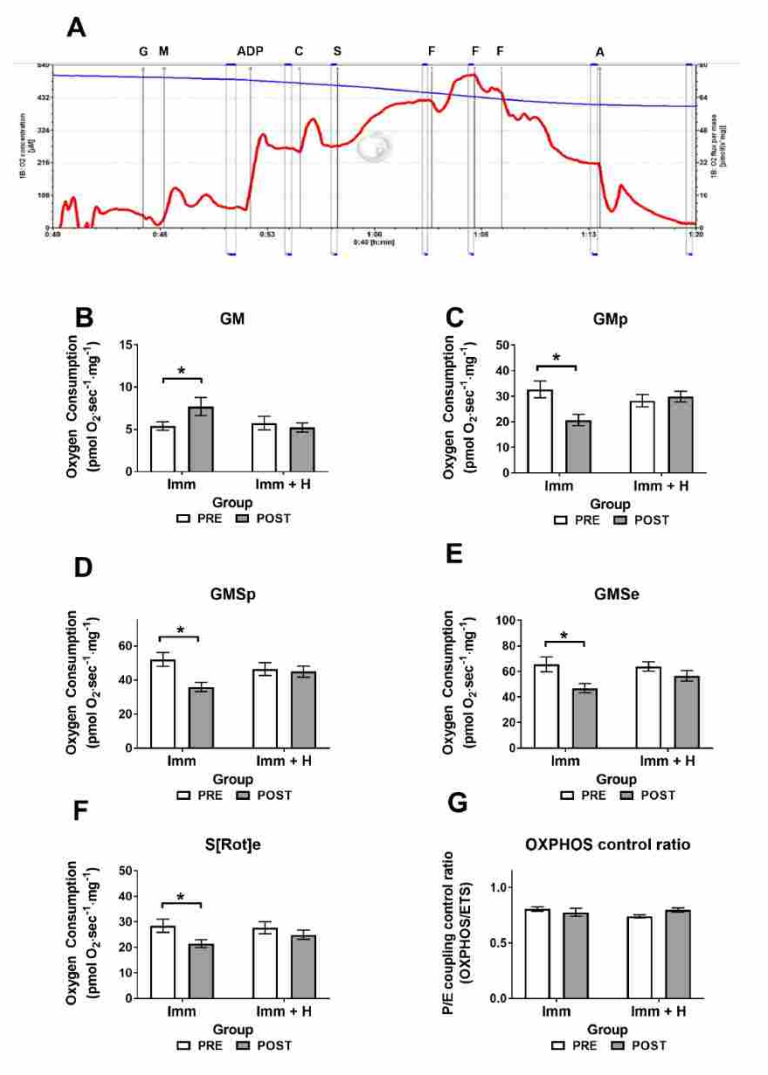


Figure 2.3. Mitochondrial respiratory capacity. Respiratory capacity decreased after 10 days of immobilization (Imm), but was rescued with daily heating (Imm + H). **(A)** Representative respiratory run following the standard SUIT protocol with stepwise additions of Glutamate (G), Malate (M), ADP, Succinate (S), FCCP (F) uncoupler, and Antimycin A (A). Individual graphs for **(B)** Leak; GM, **(C)** Complex I-mediated; GMp **(D)** Maximal-coupled; GMSp, **(E)** Maximal-uncoupled; GMSe, and **(F)** Complex II-uncoupled; S[Rot]e respiratory capacity. **(G)** OXPHOS control ratio (GMSp/GMSe) was not changed following immobilization. *$p < 0.05$, significant change from baseline (pre). Data are mean ± SEM, n = 19-21.

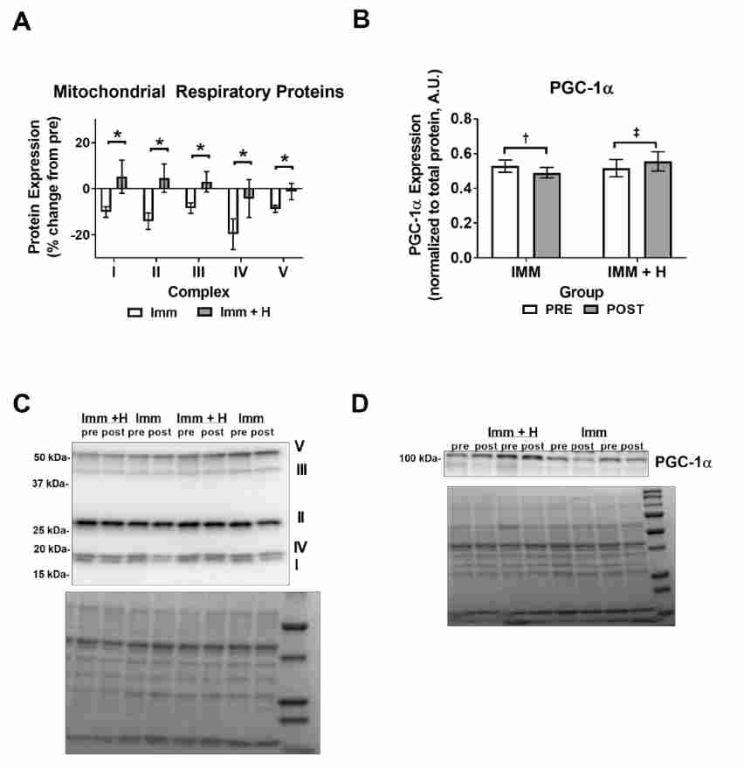


Figure 2.4. Mitochondrial respiratory protein expression. Mitochondrial respiratory protein and PGC-1α expression decreased with immobilization only (Imm), but not after immobilization with daily heat therapy (Imm + H). **(A)** Expression of proteins for each of the 5 respiratory complexes decreased with Imm, but not Imm + H. **(B)** PGC-1α expression decreased with Imm, but increased with Imm + H. Representative blots and Ponceau Red stains for **(C)** total OXPHOS and **(D)** PGC-1α. *$p < 0.05$, significant difference between groups. †$p < 0.05$, significant decrease with Imm. ‡$p < 0.05$, significant increase for Imm + H. Data are mean ± SEM, n = 18-23.

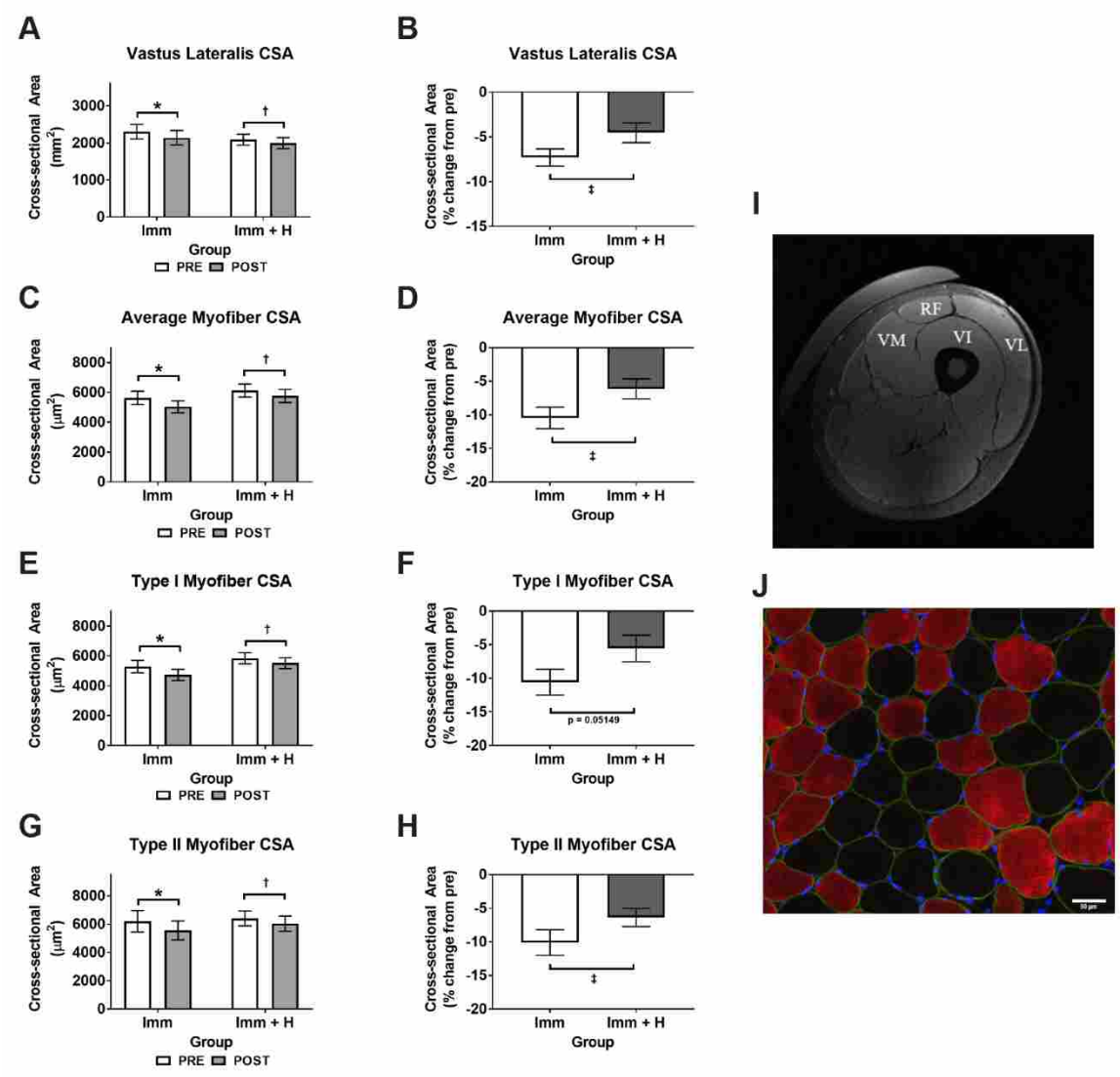


Figure 2.5. Changes in muscle cross-sectional area (CSA). CSA was decreased to a lesser extent after 10 days of immobilization with heating (Imm + H), compared to control (Imm). Decreases in both **(A & B)** whole-muscle CSA of the vastus lateralis, and **(C-H)** myofiber CSA were attenuated with heating. **(I)** Representative MRI image with all 4 quadriceps muscles labeled (VM- vastus medialis, RF- rectus femoris, VI-vastus intermedius, VL-vastus lateralis). Note the silicone mold on the top of the quadriceps to mark the plane of heating. **(J)** Representative image of myofiber staining (blue- DAPI, green- dystrophin, red- MHC I). *$p < 0.05$, significant decrease with Imm. †$p < 0.05$, significant decrease with Imm + H. ‡$p < 0.05$, significant difference between groups. Data are mean ± SEM, n = 17-20.

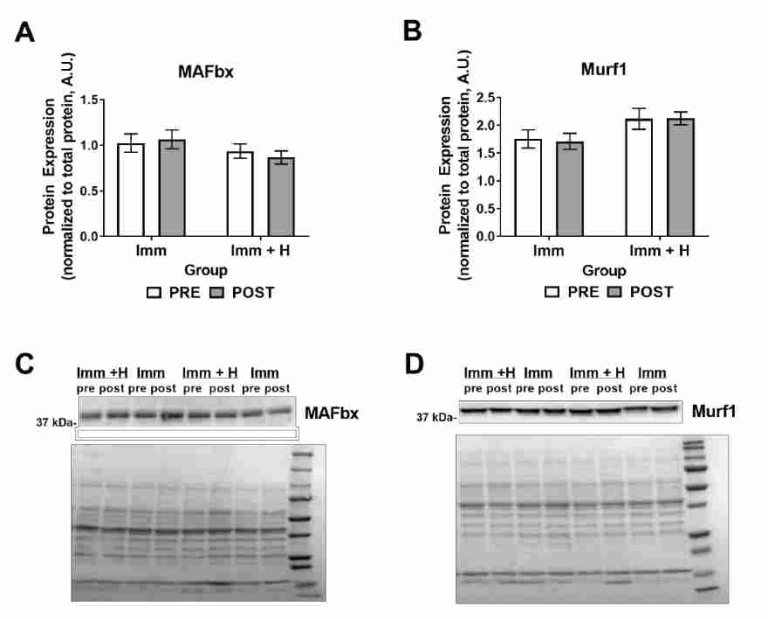


Figure 2.6. E3 Ubiquitin Ligases. Ligases were unchanged with immobilization (Imm) and heating (Imm + H). **(A)** MAFbx and **(B)** Murf1. Representative blots and Ponceau Red stains for **(C)** MAFbx and **(D)** Murf1. Data are mean ± SEM, n = 22-23.

References


1. **Abadi A, Glover EI, Isfort RJ, Raha S, Safdar A, Yasuda N, Kaczor JJ, Melov S, Hubbard A, Qu X, Phillips SM, Tarnopolsky M.** Limb immobilization induces a coordinate down-regulation of mitochondrial and other metabolic pathways in men and women. *PLoS ONE* 4(8): e6518, 2009.
2. **Akimoto T, Pohnert SC, Li P, Zhang M, Gumbs C, Rosenberg PB, Williams RS, Yan Z.** Exercise Stimulates PGC-1α Transcription in Skeletal Muscle through Activation of the p38 MAPK Pathway. *J Bio1 Chem* 280(20): 19587-19593, 2005.
3. **Barone R, Macaluso F, Sangiorgi C, Campanella C, Gammazza AM, Moresi V, Coletti D, Macario EC, Macario AJL, Cappello F, Adamo S, Farina F, Zummo G, Di Felice V.** Skeletal muscle heat shock protein 60 increases after endurance training and induces peroxisome proliferator-activated receptor gamma coactivator 1 α1 expression. *Sci Reports* 6: 19781, 2016.
4. **Blomstrand E, Radegran G, Saltin B.** Maximum rate of oxygen uptake by human skeletal muscle in relation to maximal activities of enzymes in the Krebs cycle. *J Physiol* 501(2): 455-460, 1997.
5. **Bodine SC, Latres E, Baumhueter S, Lai VK, Nunez L, Clarke BA, Poueymirou WT, Panaro FJ, Na E, Dharmarajan K, Pan ZQ, Valenzuela DM, DeChiara TM, Stitt TN, Yancopoulos GD, Glass DJ**. Identification of ubiquitin ligases required for skeletal muscle atrophy. *Science* 294: 1704-1708, 2001.
6. **Brault JJ, Jespersen JG, Goldberg AL.** Peroxisome proliferator-activated receptor γ coactivator 1α or 1β overexpression inhibits muscle protein degradation, induction of ubiquitin ligases, and disuse atrophy. *J Biol Chem* 285(25): 19460-19471, 2010.
7. **Brocca L, Cannavino J, Coletto L, Biolo G, Sandri M, Bottinelli R, Pelligrino MA**. The time course of the adaptations of human muscle proteome to bed rest and the underlying mechanisms. *J Physiol* 590(20): 5211-5230, 2012.
8. **Brooks GA, Hittelman KJ, Faulkner JA, Beyer RE.** Tissue temperatures and whole-animal oxygen consumption after exercise. *Am J Physiol* 221: 427-431, 1971.
9. **Canto C, Auwerx J.** Calorie restriction: is AMPK a key sensor and effector? *Physiology (Bethesda)* 26(4): 214-224, 2011.
10. **Chapman MA, Meza R, Lieber RL**. Skeletal muscle fibroblasts in health and disease. *Differentiation* 92: 108-115, 2016.
11. **Chen YW, Gregory CM, Scarborough MT, Shi R, Walter GA, Vandenborne K.** Transcriptional pathways associated with skeletal muscle disuse atrophy in humans. *Physiol Genomics* 31: 510-520, 2007.
12. **Cortright RN, Zheng D, Jones JP, Fluckey JD, DiCarlo SE, Grujic D, Lowell BB, Dohm GL.** Regulation of skeletal muscle UCP-2 and UCP-3 gene expression by exercise and denervation. *Am J Physiol Endocrinol Metab* 276(39): E217-E221, 1999.
13. **De Boer MD, Selby A, Atherton P, Smith K, Seynnes OR, Maganaris CN, Maffulli N, Movin T, Narici MV, Rennie MJ.** The temporal responses of protein synthesis, gene expression and cell signaling in human quadriceps muscle and patellar tendon to disuse. *J Physiol* 585(1): 241-251, 2007.
14. **De Maio A, Santoro G, Tanguay RM, Hightower LE.** Ferruccio Ritossa's scientific legacy 50 years after his discovery of the heat shock response: a new view of biology, a new society, and a new journal. *Cell Stress and Chaperones* 17: 139-143, 2012.

15. **Dirks ML, Wall BT, Snijders T, Ottenbros CLP, Verdijk LB, van Loon LJC**. Neuromuscular electrical stimulation prevents muscle disuse atrophy during leg immobilization in humans. *Acta Physiol* 210(3): 628-41, 2013.
16. **Dodd SL, Hain B, Senf SM, Judge AR.** HSP27 inhibits IKKβ-induced NF-κB activity and skeletal muscle atrophy. *FASEB J* 23: 3415-3423, 2009.
17. **Draper DO, Harris ST, Schulthies S, Durrant E, Knight KL, Ricard M.** Hot-pack and 1-MHz ultrasound treatments have an additive effect on muscle temperature increases. *J Athl Training* 33(1): 21-24, 1998.
18. **Draper DO, Hawkes AR, Johnson AW, Diede MT, Rigby JH.** Muscle heating with Megapulse II shortwave diathermy and ReBound diathermy. *J Athl Training* 48(4): 477-482, 2013.
19. **Feletou M, Vanhoutte PM.** EDHF: an update. *Clin Sci* 117: 139-155, 2009.
20. **Foletta VC, White LJ, Larsen AE, Leger B, Russell AP.** The role and regulation of MAFbx/atrogin-1 and MuRF1 in skeletal muscle atrophy. *Pflugers Arch* 461: 325-335. 2011.
21. **Gibson JNA, Halliday D, Morrison WL, Stoward PJ, Hornsby GA, Watt PW, Murdoch G, Rennie MJ.** Decrease in human quadriceps muscle protein turnover consequent upon leg immobilization. *Clin Sci* 72: 503-509, 1987.
22. **Giombini A, Giovannini V, Di Cesari A, Pacetti P, Ichinoseki-Sekine N, Shiraishi M, Naito H, Maffulli N.** Hyperthermia induced by microwave diathermy in the management of muscle and tendon injuries. *Br Med Bulletin* 83: 379-396, 2007.
23. **Glover EI, Phillips SM, Oates BR, Tang JE, Tarnopolsky MA, Selby A, Smith K, Rennie MJ.** Immobilization induces anabolic resistance in human myofibrillar protein synthesis with low and high dose amino acid infusion. *J Physiol* 586(24): 6049-6061, 2008.
24. **Glover EI, Yasuda N, Tarnopolsky MA, Abadi A, Phillips SM.** Little change in markers of protein breakdown and oxidative stress in humans in immobilization-induced skeletal muscle atrophy. *Appl Physiol Nutr Metab* 35: 125-133, 2010.
25. **Gnaiger E.** Capacity of oxidative phosphorylation in human skeletal muscle: New perspectives of mitochondrial physiology. *Int J Biochem Cell Biol* 41**:** 1837-1845, 2009.
26. **Gram M, Vigelso A, Yokata T, Hansen CN, Helge JW, Hey-Mogensen M, Dela F**. Two weeks of one-leg immobilization decreases skeletal muscle respiratory capacity equally in young and elderly men. *Experiment Geront* 58: 269-278, 2014.
27. **Henstridge DC, Bruce CR, Drew BG, Tory K, Kolonics A, Estevez E, Chung J, Watson N, Gardner T, Young RS, Connor T, Watt MJ, Carpenter K, Hargreaves M, McGee SL, Hevener AL, Febbraio MA.** Activating HSP72 in rodent skeletal muscle increases mitochondrial number and oxidative capacity and decreases insulin resistance. *Diabetes* 63: 1881-1894, 2014.
28. **Hollander JM, Martin JL, Belke DD, Scott BT, Swanson E, Krishnamoorthy V, Dillmann WH.** Overexpression of wild-type Heat shock protein 27 and a nonphosphorylatable heat shock protein 27 mutant protects against ischemia/ reperfusion injury in a transgenic mouse model. *Circulation* 110: 3544-3552, 2004.
29. **Holloszy JO, Coyle EF.** Adaptations of skeletal muscle to endurance exercise and their metabolic consequences. *J Appl Physiol Respirat Environ Exercise Physiol* 56(4): 831-838, 1984.

30. **Holloszy JO.** Biochemical adaptations in muscle: effects of exercise on mitochondrial oxygen uptake and respiratory enzyme activity in skeletal muscle. *J Biol Chem* 242(9): 2278-2282, 1967.
31. **Hood DA, Uguccioni G, Vainshtein V, D'souza D.** Mechanisms of exercise-induced mitochondrial biogenesis in skeletal muscle: implications for health and disease. *Compr Physiol* 1: 1119-1134, 2011.
32. **Hooper PL.** Hot-tub therapy for type 2 diabetes mellitus. *N Engl J Med* 341: 924-925, 1999.
33. **Jackman RW, Kandarian SC.** The molecular basis of skeletal muscle atrophy. *Am J Physiol Cell Physiol* 287: C834-C843. 2004.
34. **Jackson A, Friedman S, Zhan X, Engleka KA, Forough R, Maciag T**. Heat shock induces the release of fibroblast growth factor 1 from NIH 3T3 cells. *Proc Natl Acad Sci* 89: 10691-10695, 1992.
35. **Jones SW, Hill RJ, Krasney PA, O'Conner B, Peirce N, Greenhaff PL.** Disuse atrophy and exercise rehabilitation in humans profoundly affects the expression of genes associated with the regulation of skeletal muscle mass. *FASEB J* 18(9): 1025-1027, 2004.
36. **Julienee CM, Dumas JF, Goupille C, Pinault M, Berri C, Collin A, Tesseraud S, Couet C, Servais S.** Cancer cachexia is associated with a decrease in skeletal muscle mitochondrial oxidative capacities without alteration of ATP production efficiency. *J Cachexia Sarcopenia Muscle* 3: 265-275, 2012.
37. **Kim MY, Lee JU, Kim JH, Lee LK, Park BS, Yang SM, Jeon HJ, Lee WD, Noh JW, Kwak TY, Jang SH, Lee TH, Kim JY, Kim B, Kim J.** Phosphorylation of heat shock protein 27 is increased by cast immobilization and by serum-free starvation in skeletal muscles. *J Phys Ther Sci* 26: 1975-1977, 2014.
38. **Kregel KC.** Heat shock proteins: modifying factors in physiological stress responses and acquired thermotolerance. *J Appl Physiol* 92(5): 2177-2186, 2002.
39. **Ku Z, Yang J, Menon V, Thomason DB.** Decreased polysomal HSP-70 may slow polypeptide elongation during skeletal muscle atrophy. *Am J Physiol Cell Physiol* 268: C1369-74, 1995.
40. **Larsen S, Nielsen J, Hansen CN, Nielsen LB, Wibrand F, Stride N, Schroder HD, Boushel R, Helge JW, Dela F, Hey-Mogensen M.** Biomarkers of mitochondrial content in skeletal muscle of healthy young human subjects. *J Physiol* 590(14): 3349-3360, 2012.
41. **Leger B, Vergani L, Soraru G, Hespel P, Derave W, Gobelet C, D'Ascenzio C, Angelini C, Russell AP.** Human skeletal muscle atrophy in amyotrophic lateral sclerosis reveals a reduction in Akt and an increase in atrogin-1. *FASEB J* 20(3): 583-585, 2006
42. **Li GC, Werb Z.** Correlation between synthesis of heat shock proteins and development of thermotolerance in Chinese hamster fibroblasts. *Proc Natl Acad Sci* 79: 3218-3222, 1982.
43. **Liu CC, Lin CH, Lin CY, Lee CC, Lin MT, Wen HC.** Transgenic overexpression of heat shock protein 72 in mouse muscle protects against exhaustive exercise-induced skeletal muscle damage. *J Form Med Assoc* 112(1): 24-30, 2013.
44. **Liu CT, Brooks GA.** Mild heat stress induces mitochondrial biogenesis in C2C12 myotubes. *J Appl Physiol* 112: 354-361, 2012.
45. **Liu NF, Olszewski W**. The influence of local hyperthermia on lymphedema and lymphedematous skin of the human leg. *Lymphology* 26: 28-37, 1993.

46. **Mancini DM, Walter G, Reichek N, Lenkinski R, McCully KK, Mullen JL, Wilson JR.** Contribution of skeletal muscle atrophy to exercise intolerance and altered muscle metabolism in heart failure. *Circulation* 85: 1364-1373, 1992.
47. **Marsin AS, Bertrand L, Rider MH, Deprez J, Beauloye C, Vincent MF, Van den Berge G, Carling D, Hue L.** Phosphorylation and activation of heart PFK-2 by AMPK has a role in the stimulation of glycolysis during ischaemia. *Curr Biol* 10(20): 1247-1255, 2000.
48. **McArdle A, Dillmann WH, Mestril R, Faulkner JA, Jackson MJ.** Overexpression of HSP70 in mouse skeletal muscle protects against muscle damage and age-related muscle dysfunction. *FASEB J* 18(2): 1-12, 2004.
49. **Min K, Smuder AJ, Kwon O, Kavazis AN, Szeto HH, Powers SK.** Mitochondrial-targeted antioxidants protect skeletal muscle against immobilization-induced muscle atrophy. *J Appl Physiol* 111: 1459-1466, 2011.
50. **Montilla SIR, Johnson TP, Pearce SC, Salmon D, Gabler NK, Ross JW, Rhoads RP, Baumgard LH, Lonergan SM, Selsby JT.** Heat stress causes oxidative stress but not inflammatory signaling in porcine skeletal muscle. *Temperature* 1(1): 42-50, 2014.
51. **Morgensen M, Sahlin K, Fernstrom M, Glintborg D, Vind BF, Beck-Nielsen H, Hojlund K.** Mitochondrial respiration is decreased in skeletal muscle of patients with type 2 diabetes. *Diabetes* 56: 1592-1599, 2007.
52. **Moseley PL.** Heat shock proteins and heat adaptation of the whole organism. *J Appl Physiol* 83(5): 1413-1417, 1997.
53. **Mukai R, Matsui N, Fujikara Y, Matsumoto N, Hou DX, Kanzaki N, Shibata H, Horikawa M, Iwasa K, Hirasaka K, Nikawa T, Terao J.** Preventive effect of dietary quercetin on disuse muscle atrophy by targeting mitochondria in denervated mice. *J Nutr Biochem* 31: 67-76, 2016.
54. **Mulligan JD, Gonzalez AA, Stewart AM, Carey HV, Saupe KW.** Upregulation of AMPK during cold exposure occurs via distinct mechanisms in brown and white adipose tissue of the mouse. *J Physiol* 580: 677-684, 2007.
55. **Naito H, Powers Sk, Demirel HA, Sugiura T, Dodd SL, Aoki J.** Heat stress attenuates skeletal muscle atrophy in hindlimb-unweighted rats. *J Appl Physiol* 88: 359-363, 2000.
56. **Nelson RJ, Ziegelhoffer T, Nicolet C, Werner-Washburne M, Craig EA.** The translation machinery and 70 kd heat shock protein cooperate in protein synthesis. *Cell* 71: 97-105, 1992.
57. **Ng DC, Bogoyevitch MA.** The mechanisms of heat shock activation of ERK mitogen-activated protein kinases in the interleukin 3-dependent ProB cell line BaF3. *J Biol Chem* 275(52): 40856-40866, 2000.
58. **Ojuka EO, Jones TE, Han D, Chen M, Wamhoff BR, Sturek M, Holloszy JO**. Intermittent increases in cytosolic $Ca^{2+}$ stimulate mitochondrial biogenesis in muscle cells. *Am J Physiol Endocrinol Metab* 283: E1040-E1045, 2002.
59. **Pedersen CB, Gregersen N.** Stress response profiles in human fibroblasts exposed to heat shock or oxidative stress. *Methods Mol Biol* 648: 161-173, 2010.
60. **Pfeffer G, Chinnery PF.** Diagnosis and treatment of mitochondrial myopathies. *Ann Med* 45: 4-16, 2013.
61. **Porter C, Reidy PT, Bhattarai N, Sidossis LS, Rasmussen BB.** Resistance exercise training alters mitochondrial function in human skeletal muscle. *Med Sci Sports Exerc* 47(9): 1922-1931, 2015.

62. **Radak Z, Chung HY, Koltai E, Taylor AE, Goto S.** Exercise, oxidative stress and hormesis. *Ageing Research Reviews* 7: 34-42, 2008.
63. **Ritov VB, Menshikova EV, Kazuma K, Wood R, Toledo FG, Goodpaster BH, Ruderman NB, Kelley DE.** Deficiency of electron transport chain in human skeletal muscle mitochondria in type 2 diabetes mellitus and obesity. *Am J Physiol Endocrinol Metab* 298: E49-E58, 2010.
64. **Romanello V, Guadagnin E, Gomes L, Roder I, Sandri C, Petersen Y, Milan G, Masiero E, Del Piccolo P, Foretz M, Scorrano L, Rudolf R, Sandri M.** Mitochondrial fission and remodeling contributes to muscle atrophy. *EMBO J* 29: 1774-85, 2010.
65. **Ronda AC, Vasconsuelo A, Boland R.** 17beta-estradiol protects mitochondrial functions through extracellular-signal-regulated kinase in C2C12 muscle cells. *Cell Physiol Biochem* 32(4): 1011-1023, 2013.
66. **Russell AP, Foletta VC, Snow RJ, Wadley GD.** Skeletal muscle mitochondria: A major player in exercise, health and disease. *Biochimica et Biophsyica Acta* 1840**:** 1276-1284, 2014.
67. **Saltin B, Gagge AP, Stolwijk JA.** Muscle temperature during submaximal exercise in man. *J Appl Physiol* 25: 679-688, 1968.
68. **Sandri M, Lin J, Handschin C, Yang W, Arany ZP, Lecker SH, Goldberg AL, Spiegelman BM.** PGC-1α protects skeletal muscle from atrophy by suppressing FoxO3 action and atrophy-specific gene transcription. *PNAS* 103(44): 16260-16265, 2006.
69. **Sekins KM, Lehmann JF, Esselman P, Dundore D, Emergy AF, deLateur BJ, Nelp WB.** Local muscle blood flow and temperature responses to 915MHz diathermy as simultaneously measured and numerically predicted. *Arch Phys Med Rehabil* 65(1): 1-7, 1984.
70. **Senf SM, Dodd SL, McClung JM, Judge AR.** HSP70 overexpression inhibits NF-κB and Foxo3a transcriptional activities and prevents skeletal muscle atrophy. *FASEB J* 22: 3836-3845, 2008.
71. **Short KR, Bigelow ML, Kahl J, Singh R, Coenen-Schimke J, Raghavakaimal S, Nair KS.** Decline in skeletal muscle mitochondrial function with aging in humans. *PNAS* 102(15): 5618-5623, 2005.
72. **Siddique YS, Ara G, Afzal M.** Estimation of lipid peroxidation induced by hydrogen peroxide in cultured human lymphocytes. *Dose-Response* 10(1): 1-10, 2012.
73. **Spina RJ, Chi MM, Hopkins MG, Nemeth PM, Lowry OH, Holloszy JO.** Mitochondrial enzymes increase in muscle in response to 7-10 days of cycle exercise. *J Appl Physiol* 80(6): 2250-2254, 1996.
74. **Spinazzi M, Casarin A, Peregato V, Salviati L, Angelini C.** Assessment of mitochondrial respiratory chain enzymatic activities on tissues and cultured cells. *Nature Protocols* 7(6): 1235-1246, 2012.
75. **Tamura Y, Kitaoka Y, Matsunaga Y, Hoshino D, Hatta H.** Daily heat stress treatment rescues denervation-activated mitochondrial clearance and atrophy in skeletal muscle. *J Physiol* 593(12): 2707-2720, 2015.
76. **Tamura Y, Matsunaga Y, Masuda H, Takahashi YUM, Takahashi YUK, Terada S, Hoshino D, Hatta H.** Postexercise whole body heat stress additively enhances endurance training-induced mitochondrial adaptations in mouse skeletal muscle. *Am J Physiol Regul Integr Comp Physiol* 307: R931-R943, 2014.

77. **Tarnopolsky MA, Raha S.** Mitochondrial myopathies: diagnosis, exercise intolerance, and treatment options. *Med Sci Sports Exerc* 37(12): 2086-2093, 2005.
78. **Thom JM, Thompson MW, Ruell PA, Bryant GJ, Fonda JS, Harmer AR, Janse de Jonge XA, Hunter SK.** Effect of 10-day cast immobilization on sarcoplasmic reticulum calcium regulation in humans. *Acta Physiol Scand* 172: 141-147, 2001.
79. **Thomason DV.** Translational control of gene expression in muscle. *Exerc Sport Sci Res* 26: 165-190, 1998.
80. **Touchberry C, Le T, Richmond S, Prewitt M, Beck D, Carr D, Vardiman P, Gallagher P.** Diathermy treatment increases heat shock protein expression in female, but not male skeletal muscle. *Eur J Appl Physiol* 102: 319-323, 2008.
81. **Tsuchida W, Iwata M, Akimoto T, Matsuo S, Asai Y, Suzuki S.** Heat stress modulates both anabolic and catabolic signaling pathways preventing dexamethasone-induced muscle atrophy in vitro. *J Cell Physiol* 232(3): 650-664, 2017.
82. **Urso ML, Scrimgeour AG, Chen YW, Thompson PD, Clarkson PM.** Analysis of human skeletal muscle after 48 h immobilization reveals alterations in mRNA and protein for extracellular matrix components. *J Appl Physiol* 101: 1136-1148, 2006.
83. **Vidyasagar A, Wilson NA, Djamali A.** Heat shock protein 27 (HSP27): biomarker of disease and therapeutic target. *Fibro Tiss Repair* 5(7):1-7, 2012.
84. **Winder WW, Holmes BF, Rubink DS, Jensen EB, Chen M, Holloszy JO.** Activation of AMP-activated protein kinase increases mitochondrial enzymes in skeletal muscle. *J Appl Physiol* 88: 2219-2226, 2000.
85. **Wiper DJ, McNiven DR**. The effect of microwave therapy upon muscle blood flow in man. *Br J Sports Med* 10: 19-21, 1976.
86. **Wolfe RR.** The underappreciated role of muscle in health and disease. *Am J Clin Nutr* 84: 475-482, 2006.
87. **Yasuda N, Glover EI, Phillips SM, Isfort RJ, Tarnopolsky MA.** Sex-based differences in skeletal muscle function and morphology with short-term limb immobilization. *J Appl Physiol* 99: 1085-1092, 2005.
88. **Zou MH, Kirkpatrick SS, Davis BJ, Nelson JS, Wiles 4th WG, Schlattner U, Neumann D, Brownlee M, Freeman MB, Goldman MH.** Activation of the AMP-activated protein kinase by the anti-diabetic drug metformin in vivo. Role of mitochondrial reactive nitrogen species. *J Biol Chem* 279(42): 43940-43951, 2004.